

Low-dimensional q -tori in FPU lattices: dynamics and localization properties

H. Christodoulidi^a, C. Efthymiopoulos^b,

^a Università degli Studi di Padova,

Dipartimento di Matematica Pura e Applicata,

Via Trieste 63, 35121 - Padova, Italy

^b Research Center for Astronomy and Applied Mathematics,
Academy of Athens, Greece

March 12, 2019

Abstract

This is a continuation of our study in [10] concerning q -tori, i.e. low-dimensional tori in the phase space of nonlinear lattice models like the Fermi-Pasta-Ulam (FPU). In [10] we focused on the FPU- β system, and we showed that the dynamical features of the q -tori serve as an interpretational tool to understand phenomena of *energy localization* in the FPU space of linear normal modes (q -space). In the present paper we compute quasi-periodic q -tori solutions in the α model as well, using the method of Poincaré – Lindstedt series. Then, we study the localization features of the q -tori solutions in both the α and β models. We consider various so-called ‘initial excitations’. These are different choices of subsets of modes to which we give a non-zero oscillation amplitude at 0-th order of perturbation theory. We focus on two classes of initial excitations: i) ones describing low-frequency ‘packets’ of modes, and ii) excitations of a (small) set of modes with an arbitrary distribution in q -space. In the former case, we find formulae yielding an exponential profile of energy localization, following an analysis of the size of the leading order terms in the Poincaré – Lindstedt series. In the latter case, we explain the observed localization patterns on the basis of a rigorous result concerning the propagation of non-zero terms in the Poincaré – Lindstedt series from zero to subsequent orders. In both cases, the resulting localization patterns are found to agree to a large extent with the corresponding metastable states for so-called ‘FPU-trajectories’, which have initial conditions close to q -torus solutions. However, we also discuss some differences between q -tori solutions and FPU-trajectories with similar localization profiles. Finally, we discuss the extensive (i.e. independent of the number of degrees of freedom) properties of some q -tori solutions.

1 Introduction

In a recent paper [10] we introduced the concept of q -tori in the space of normal modes (q -space) of the Fermi – Pasta – Ulam model [1] described by a quadratic potential of nearby particle interactions plus a quartic perturbation (FPU- β). A q -torus is an invariant torus hosting quasi-periodic trajectories whose limit, for $\beta = 0$, reduces to the product of more than one independent normal mode oscillations. In [10] the existence of q -tori was studied in a Cantor set in phase space, using the method of *Poincaré - Lindstedt (PL) series*. Furthermore, we examined in detail the case of q -tori whose dimension is much smaller than the number of degrees of freedom N . Such tori were found relevant to interpreting the phenomenon of *energy localization*, which is observed in FPU trajectories resulting from particular classes of initial conditions. According to this, we observe that, if energy is given initially to a small set of low-frequency modes, the flow of energy from the initial to the remaining modes may appear ‘frozen’ for quite long times, resulting in the system exhibiting important deviations from energy equipartition. Energy localization is characterized by the formation of a so-called ‘metastable state’ [12, 13, 20, 21, 22]. A main feature of such a state is the appearance of an approximate ‘plateau’ in the low-frequency part of the energy spectrum E_q (a so-called ‘natural packet’ of modes [14, 17, 18]), accompanied by an exponential tail of the energy distribution for the remaining modes. Important problems concern the dependence of a packet’s width s on the specific energy $\varepsilon = E/N$ given to a system (where E is the total energy), as well as the dependence of the time T , up to which a metastable state persists, on ε . A state-of-the-art account of numerical facts related to these problems is given in [19], containing also many references to earlier works. Briefly, numerical experiments indicate that the functions $s(\varepsilon)$ and $T(\varepsilon)$ behave differently in the α and in the β -FPU models, depending also on the precise form as well as on the degree of phase coherence of the initial conditions characterizing packet excitation (see also the review [16]).

Another concept related to q -tori is the concept of q -breathers, introduced in the series of works [3]–[9]. The q -breathers are periodic orbits, whose localization profiles share many common features with those of particular q -tori solutions. In fact, a q -breather can be considered as a one-dimensional q -torus. Contrary to q -tori, however, the existence of q -breathers is guaranteed by basic theorems on the continuation of periodic orbits from linear to non-linearly perturbed systems. On the other hand, the q -tori effectively describe a wider class of initial excitations in the FPU problem than the q -breathers. Thus, q -tori and q -breathers should be regarded as complementary interpretational tools of FPU localization phenomena. Further comparison is deferred to section 3.4.

In a paper accompanying the present one [11], we explain in detail the numerical procedure by which we locate the q -tori, and we discuss the convergence properties of the corresponding PL series. In the present paper, on the other hand, we mainly focus on the physical aspects of our study. In particular, we seek to explain theoretically the energy localization properties observed in q -tori. To this end, we explore a concept introduced already in [10], namely the so-called propagation of ‘initial excitations’ in the PL series terms. In the context of PL series, an ‘initial excitation’ means a particular selection of a subset of modes in q -space for which we consider an oscillation with non-zero amplitude at the 0-th order of perturbation theory. Then, this excitation ‘propagates’ to new modes at subsequent orders. Similarly to the β case considered in [10], in section 2 we prove a general proposition regarding the pattern of this propagation, applicable to both the α and β models.

The latter proposition is exploited, in turn, in order to predict theoretically the form of energy localization profiles depending on the initial excitation. In section 3, we study such profiles and compare them with the profiles of FPU-trajectories arising from the energy given initially exclusively to a few modes (this is in contrast to the q -tori solutions in which all modes have initially some, albeit possibly quite small, energy). Our numerical evidence is that the localization profiles of q -tori and nearby FPU-trajectories are very similar. In the case of ‘extensive’ initial excitations (i.e. ones where the number of initially excited modes varies proportionally to N), we predict that the form of the energy spectrum corresponding to a

given localization profile depends only on the specific energy $\varepsilon = E/N$. Furthermore, we find approximative formulae for the form of localization profiles corresponding to various arbitrary choices of the set q_i , $i = 1, \dots, s$ of initially excited modes, based on a leading term analysis of the associated PL series. In the case of low-frequency packets these profiles are exponential, with a slope depending *logarithmically* on the system's parameters. We also study the case of q -breathers, where a similar law is found in [7], when the so-called 'seed mode' q_0 is taken to vary proportionally to N . All these results are verified in numerical computations.

Section 4 is a summary of our basic conclusions from the present study and a discussion on future perspectives.

2 Analytic construction of q -tori

2.1 The Fermi Pasta Ulam model

The FPU Hamiltonian for a lattice of $N - 1$ particles reads:

$$H = \frac{1}{2} \sum_{k=1}^{N-1} y_k^2 + \frac{1}{2} \sum_{k=0}^{N-1} (x_{k+1} - x_k)^2 + \frac{\alpha}{3} \sum_{k=0}^{N-1} (x_{k+1} - x_k)^3 + \frac{\beta}{4} \sum_{k=0}^{N-1} (x_{k+1} - x_k)^4 \quad (1)$$

where x_k is the k -th particle's position with respect to equilibrium and y_k its canonically conjugate momentum. Fixed boundary conditions are defined by setting $x_0 = x_N = 0$. The cases $\alpha \neq 0, \beta = 0$, and $\alpha = 0, \beta \neq 0$ are called FPU- α and FPU- β model respectively.

The normal mode canonical variables (Q_q, P_q) are introduced by the linear canonical transformation

$$\begin{aligned} x_k &= \sqrt{\frac{2}{N}} \sum_{q=1}^{N-1} Q_q \sin\left(\frac{qk\pi}{N}\right) \\ y_k &= \sqrt{\frac{2}{N}} \sum_{q=1}^{N-1} P_q \sin\left(\frac{qk\pi}{N}\right). \end{aligned} \quad (2)$$

Substitution of (2) into (1) yields the Hamiltonian in the normal mode space (' q -space'):

$$\begin{aligned} H &= \frac{1}{2} \sum_{q=1}^{N-1} (P_q^2 + \Omega_q^2 Q_q^2) + \frac{\alpha}{3\sqrt{2N}} \sum_{q,l,m=1}^{N-1} B_{qlm} \Omega_q \Omega_l \Omega_m Q_q Q_l Q_m \\ &+ \frac{\beta}{8N} \sum_{q,l,m,n=1}^{N-1} C_{qlmn} \Omega_q \Omega_l \Omega_m \Omega_n Q_q Q_l Q_m Q_n \end{aligned} \quad (3)$$

with normal mode frequencies

$$\Omega_q = 2 \sin\left(\frac{q\pi}{2N}\right), \quad 1 \leq q \leq N-1 \quad . \quad (4)$$

The harmonic energy E_q of each normal mode q is given by

$$E_q = \frac{1}{2} (P_q^2 + \Omega_q^2 Q_q^2) \quad . \quad (5)$$

The coefficients B_{qlm} and C_{qlmn} are non-zero only for particular combinations of the indices q, l, m, n , namely

$$\begin{aligned} B_{qlm} &= \sum_{\pm} (\delta_{q\pm l\pm m, 0} - \delta_{q\pm l\pm m, 2N}) \\ C_{qlmn} &= \sum_{\pm} (\delta_{q\pm l\pm m\pm n, 0} - \delta_{q\pm l\pm m\pm n, 2N}) . \end{aligned} \quad (6)$$

In the above expressions, all possible combinations of the \pm signs must be taken into account. In the new canonical variables, the equations of motion are:

$$\begin{aligned} \ddot{Q}_q + \Omega_q^2 Q_q &= -\frac{\alpha}{\sqrt{2N}} \sum_{l,m=1}^{N-1} B_{qlm} \Omega_q \Omega_l \Omega_m Q_l Q_m \\ &\quad - \frac{\beta}{2N} \sum_{l,m,n=1}^{N-1} C_{qlmn} \Omega_q \Omega_l \Omega_m \Omega_n Q_l Q_m Q_n . \end{aligned} \quad (7)$$

2.2 Construction of q -tori by Poincaré–Lindstedt series

As a starting point for the construction of quasi-periodic solutions lying on ‘ q -tori’, we consider first the trivial case $\alpha = \beta = 0$. Let

$$\mathcal{D}_0 \equiv \{q_1, q_2, \dots, q_s\}, \quad \text{where } 1 \leq q_i \leq N-1 \text{ with } q_i < q_j, \text{ for } i < j$$

be an arbitrary set of $s < N$ modes, called hereafter ‘seed modes’ (in analogy to [3], where the case $s = 1$ corresponding to q -breathers is considered). The set of functions $Q_{q_i}(t) = A_{q_i} \cos(\Omega_{q_i} t + \phi_{q_i})$, $i = 1, \dots, s$ and $Q_q(t) = 0$ if $q \notin \mathcal{D}_0$, constitutes a particular solution of the linear system. The resulting trajectory lies on an s -dimensional torus, provided that the frequencies Ω_{q_i} of Eq. (4) satisfy no commensurability relation. This turns out to be always the case if $N-1$ is a prime number or $\log_2 N \in \mathbf{N}^*$ [26]. If, on the other hand, the frequencies Ω_{q_i} satisfy s' linearly independent commensurability relations ($0 < s' < s$), the trajectories lie on a ‘resonant torus’ of dimension $s - s'$, which is a sub-manifold of the original q -torus of dimension s .

Passing now to the nontrivial case $a \neq 0$, or $\beta \neq 0$, we aim to define quasi-periodic trajectories lying again on s -dimensional tori. To this end, let ω_{q_i} , $i = 1, \dots, s$ be a set of frequencies with fixed values *chosen in advance*, which are incommensurable between themselves as well as with each one of the linear frequencies Ω_q of the remaining modes $q \notin \mathcal{D}_0$. We then determine formal solutions $Q_q(t)$, $q = 1, \dots, N-1$ containing only trigonometric terms of the form $\cos(n \cdot (\omega t + \phi))$, where $n \equiv (n_1, n_2, \dots, n_s)$ is an s -dimensional integer vector and $\omega \equiv (\omega_{q_1}, \dots, \omega_{q_s})$, $\phi \equiv (\phi_{q_1}, \dots, \phi_{q_s})$ are the frequency and phase vectors respectively.

According to the PL method, these solutions for FPU- α or FPU- β model are written as series in powers of a small parameter $\mu = \alpha/\sqrt{2N}$, or $\mu = \beta/2N$ respectively, namely:

$$Q_q(t) = \sum_{k=0}^{\infty} \mu^k Q_q^{(k)}(t), \quad q = 1, \dots, N-1 . \quad (8)$$

The series terms $Q_q^{(k)}$ are computed step by step. The 0-th order terms are set as

$$Q_q^{(0)}(t) = \begin{cases} A_q \cos(\omega_q t + \phi_q), & \text{if } q \in \mathcal{D}_0 \\ 0, & \text{otherwise} . \end{cases} \quad (9)$$

We emphasize that the amplitudes A_{q_i} , $i = 1, \dots, s$ are unknown quantities to be specified at the end of the process. In the computer–algebraic program, A_{q_i} are symbols carried all along the construction of the PL series, while the frequencies ω_{q_i} are substituted at the beginning by their selected numerical values [11]. However, according to the PL method, the frequencies ω_{q_i} must also be expressed in the form of a series in powers of the amplitudes A_{q_i} , namely

$$\omega_{q_i} = \Omega_{q_i} + \sum_{k=1}^{\infty} \mu^k \omega_{q_i}^{(k)}(A_{q_1}, \dots, A_{q_s}) . \quad (10)$$

The functions $\omega_{q_i}^{(k)}(A_{q_1}, \dots, A_{q_s})$ are polynomials of the amplitudes A_{q_1}, \dots, A_{q_s} , of order $k + 1$ in the α -case, or $2k + 1$ in the β -case.

Substituting Eqs.(8) and (10) in the equations of motion (7), we find the following equations to be solved at order k : for the FPU- α model we have

$$\begin{aligned} \ddot{Q}_q^{(k)} + \omega_q^2 Q_q^{(k)} &= \sum_{n_1=1}^k \sum_{n_2=0}^{n_1} \omega_q^{(n_2)} \omega_q^{(n_1-n_2)} Q_q^{(k-n_1)} \\ &\quad - \Omega_q \sum_{l,m=1}^{N-1} \Omega_l \Omega_m B_{qlm} \sum_{\substack{n_1,2=0 \\ n_1+n_2=k-1}}^{k-1} Q_l^{(n_1)} Q_m^{(n_2)}, \quad \text{if } q \in \mathcal{D}_0 \\ \ddot{Q}_q^{(k)} + \Omega_q^2 Q_q^{(k)} &= -\Omega_q \sum_{l,m=1}^{N-1} \Omega_l \Omega_m B_{qlm} \sum_{\substack{n_1,2=0 \\ n_1+n_2=k-1}}^{k-1} Q_l^{(n_1)} Q_m^{(n_2)}, \quad \text{if } q \notin \mathcal{D}_0 \end{aligned} \quad (11)$$

while for the FPU- β model we have

$$\begin{aligned} \ddot{Q}_q^{(k)} + \omega_q^2 Q_q^{(k)} &= \sum_{n_1=1}^k \sum_{n_2=0}^{n_1} \omega_q^{(n_2)} \omega_q^{(n_1-n_2)} Q_q^{(k-n_1)} \\ &\quad - \Omega_q \sum_{l,m,n=1}^{N-1} \Omega_l \Omega_m \Omega_n C_{qlmn} \sum_{\substack{n_1,2,3=0 \\ n_1+n_2+n_3=k-1}}^{k-1} Q_l^{(n_1)} Q_m^{(n_2)} Q_n^{(n_3)}, \quad \text{if } q \in \mathcal{D}_0 \\ \ddot{Q}_q^{(k)} + \Omega_q^2 Q_q^{(k)} &= -\Omega_q \sum_{l,m,n=1}^{N-1} \Omega_l \Omega_m \Omega_n C_{qlmn} \sum_{\substack{n_1,2,3=0 \\ n_1+n_2+n_3=k-1}}^{k-1} Q_l^{(n_1)} Q_m^{(n_2)} Q_n^{(n_3)}, \quad \text{if } q \notin \mathcal{D}_0. \end{aligned} \quad (12)$$

By integrating either Eqs.(11) or (12), secular terms of the form $t \sin(\omega_q t)$ appear in the right hand side (when $q \in \mathcal{D}_0$), at even orders in the FPU- α and at all orders in the FPU- β . The requirement to eliminate all secular terms leads to an algebraic expression for the frequency correction terms $\omega_{q_i}^{(k)}$, $i = 1, \dots, s$. After eliminating the secular terms, direct integration of Eqs.(11) or (12) yields the solution of the series terms $Q_q^{(k)}(t)$ for all $q = 1, \dots, N - 1$.

At the end of the process, we consider Eqs.(10) as a set of algebraic equations to be solved for the amplitudes A_{q_i} . The existence of a solution for a fixed choice of frequency values ω_{q_i} , along with the convergence of the series (8) for that particular solution, constitutes a proof that a q -torus with the so chosen frequencies exists. In practice, we can hardly provide such a proof by rigorous means. Instead, we

work with a finite truncation of the series (10), which we solve numerically to determine values for the amplitudes A_{q_i} , up to the approximation of the selected truncation order. Even so, a random choice of frequency values ω_{q_i} often results in that real solutions do not exist. In order to deal with this problem, we developed a numerical algorithm by which to properly choose values for the frequencies ω_{q_i} , so as to lead to a successful determination of real amplitudes for all series terms. The same algorithm takes care of how to move in frequency space, in order to determine solutions corresponding to progressively higher and higher energy. Details on this algorithm are given in 4.

After the determination of real amplitude values A_{q_i} , we substitute these latter values in the (also truncated) series (8). This gives finite expressions representing motions on a q -torus up to a finite accuracy. However, by use of some numerical indicators (like the GALI; see [23]) we provide numerical evidence on whether a solution found by the above approach represents indeed a good approximation to a q -torus solution. In fact, the GALI indicator also allows us to probe the dimension of this torus, and check whether the latter agrees with the dimension adopted a priori in the analytic solution. Further numerical tests on the convergence of the PL series are discussed in [11].

2.3 Sequence of mode excitations

It is well known that for some special choices of initial conditions, the resulting FPU-trajectories (in both the α and β models) take place on lower dimensional invariant sub-manifolds of the FPU phase space. This is due to the existence of *discrete symmetries*, which give rise to explicit low-dimensional FPU solutions. An extensive study on such symmetries is made in [27, 28, 29] (in the latter such solutions are called ‘bushes of normal modes’). A particular case are *periodic* trajectories, arising from exciting only one of the modes $q_0 = N/3, N/2$ or $2N/3$ in the β model [2] (see also [27, 29]). Solutions like the above lead, by definition, to energy localization, since the energy remains always distributed among a small subset of modes.

On the other hand, as pointed out in the introduction, we find numerically that energy localization occurs also for sets of initial conditions not obeying any obvious or simple symmetry. We now study this phenomenon using the concept of ‘propagation’ of some initial ‘excitation’ in the PL series for low-dimensional tori. We can briefly state our main result as follows: through the study of propagation, we can define a hierarchy of groups of modes participating in a q -torus solution, such that all the modes in one group share a similar (in order of magnitude) amount of energy, while distinct groups share quite different amounts of energy. The hierarchy of these groups allows us to predict the whole localization profile via a leading order analysis of the associated PL series. However, it also allows us to characterize the *paths of energy transfer* in q -space for FPU trajectories neighboring some q -torus solution, from an initial excitation up to the moment when a metastable profile is established for the FPU-trajectories.

We now give the following definitions:

Definition 1: A mode q is said to be *excited at the n -th order of the PL scheme*, iff in the series (8) it is $Q_q^{(k)}(t) = 0$ for all $k < n$, and $Q_q^{(n)}(t) \neq 0$. In addition, $Q_q^{(n)}(t)$ is called *leading order term* of the series (8).

Definition 2: Let \mathcal{D}_0 be a set of modes excited at the 0-th order of the PL scheme according to Eqs.(9). The sequence of sets $\mathcal{D}_k, k = 1, 2, \dots$, where \mathcal{D}_k consists of modes excited at the k -th order of the PL scheme, is called *sequence of mode excitations*.

Definition 3: Let k_0 be a positive constant. We call *tail modes* with respect to k_0 the modes belonging to the set $\cup_{k \geq k_0} \mathcal{D}_k$.¹

¹In [22], studying solutions corresponding to an initial excitation of the first normal mode, tail modes were called those belonging to the last third of the spectrum. This is equivalent to state that $k_0 = [2N/3]$.

Definition 4: We call *FPU-trajectory* with initial excitation in the set of modes $\mathcal{D}_0 \equiv \{q_1, \dots, q_s\}$ the trajectory resulting from the equations of motion (7) for the set of initial conditions $Q_q(0) = A_q \cos \phi_q$, $P_q(0) = -A_q \Omega_q \sin \phi_q$, for some set of amplitudes A_q and phases ϕ_q , if $q \in \mathcal{D}_0$, and $Q_q(0) = P_q(0) = 0$ if $q \notin \mathcal{D}_0$.²

In order to determine the sequence \mathcal{D}_k produced by a particular initial excitation \mathcal{D}_0 , we first define the set

$$\Sigma^r = \{-1, +1\}^r \quad . \quad (13)$$

The elements of Σ^r are r -dimensional vectors of the form $\sigma^{(r)} = (\sigma_1, \dots, \sigma_r)$, where $\sigma_i = 1$ or -1 , $i = 1, \dots, r$. Furthermore, for an r -vector $x \equiv (x_1, \dots, x_r)$ we define $\sigma^{(r)} \cdot x$ as the Euclidean product $\sigma^{(r)} \cdot x = \sigma_1 x_1 + \dots + \sigma_r x_r$. We can now prove the following

Proposition: Let $\mathcal{D}_0 = \{q_1, q_2, \dots, q_s\}$, $1 \leq q_1 < \dots < q_s \leq N - 1$ be the set of seed modes of an initial excitation yielding a formal PL solution associated with trajectories on an s -dimensional q -torus. Let M_k be the set

$$M_k = \left\{ \left| 2 \left[\frac{|\sigma^{(r)} q^{(r)}| + N - 1}{2N} \right] N - |\sigma^{(r)} q^{(r)}| \right| : \sigma^{(r)} \in \Sigma^r, \quad q^{(r)} \in \mathcal{D}_0^r \right\} \quad (14)$$

where $r = r(k)$ with $r(k) = k + 1$ for the FPU- α model and $r(k) = 2k + 1$ for the FPU- β model. Then, the sequence of mode excitations \mathcal{D}_k corresponding to the initial choice \mathcal{D}_0 is defined by the recursive relations

$$\mathcal{D}_k = M_k \setminus \bigcup_{0 \leq j \leq k-1} \mathcal{D}_j, \quad k = 1, 2, \dots \quad (15)$$

An explicit proof of the above proposition is given in [10] for the FPU- β , and in 4 for the FPU- α . We note that $[\cdot]$ is the integer part of a number and M_k represents the set of all modes for which the right hand side of Eqs. (11) and (12) is non-zero, i.e. the modes yielding some non-zero contribution to the energy spectrum up to the k -th order of the PL series (some modes excited at previous orders up to k might also belong to M_k).

Some examples clarify the use of Eq.(15):

i) *q-breathers*: If we choose $\mathcal{D}_0 = \{q_0\}$, the so-induced PL solution corresponds to a one-dimensional torus, i.e. a periodic orbit. In this case we find:

$$\mathcal{D}_k = \{q_k\} \text{ with } q_k = \left\lfloor 2 \left[\frac{r q_0 + N - 1}{2N} \right] N - r q_0 \right\rfloor, \quad (16)$$

where $r(k) = k + 1$ in the FPU- α , or $r(k) = 2k + 1$ in the FPU- β . This rule coincides with the one given in [9] for an arbitrary seed mode q_0 . From Eq. (16) we readily find that, if q_0 is even, only even modes

²As rendered clear with specific examples below, in the case of q -tori one has in general $Q_q(0) \neq 0$ or $P_q(0) \neq 0$ for *all* $q = 1, \dots, N - 1$. In fact, for the modes belonging to the k -th set \mathcal{D}_k (see Definition 2) we have in general $Q_q(t) \simeq O(\mu^k)$ for all times t , including $t = 0$. This implies that in q -tori all modes have some energy already at $t = 0$. On the contrary, according to the Definition 4, in FPU-trajectories only the modes belonging to \mathcal{D}_0 share the total energy at $t = 0$. In that sense, the use of the term ‘excitation’ for FPU-trajectories is literal, i.e. \mathcal{D}_0 refers to the modes excited at $t = 0$. The origin of the term ‘FPU-trajectories’ is that these are trajectories with initial conditions of the same type as those considered in the original FPU paper.

become excited at subsequent orders in both the α and β models. On the other hand, if q_0 is odd, in the α model both odd and even modes become excited, while in the β model only odd modes become excited. The localization properties of solutions corresponding to q -breather excitations will be discussed in detail in section 3 below.

ii) *Example with two seed modes:* Suppose $\mathcal{D}_0 = \{q_1, q_2\} = \{3, 5\}$ for N large in FPU- α . At first order ($k = 1$) it is $r(1) = 2$. In order to determine M_1 , we consider all possible combinations of the symbols $\sigma^{(2)} \in \Sigma^2$ and $q^{(2)} \in \mathcal{D}_0^2$. These are $\{(1, 1), (1, -1), (-1, 1), (-1, -1)\}$ and $\{(3, 3), (3, 5), (5, 3), (5, 5)\}$ respectively. Then from Eq.(14) we find $M_1 = \{2, 3, 5, 6, 8, 10\}$. Since $\mathcal{D}_0 = \{3, 5\}$, from Eq.(15) we have $\mathcal{D}_1 = M_1 \setminus \mathcal{D}_0 = \{2, 6, 8, 10\}$. Repeating the above procedure for $k = 2$, we find $M_2 = \{1, 3, 5, 7, 9, 11, 13, 15\}$ and $\mathcal{D}_2 = M_2 \setminus \mathcal{D}_0 \cup \mathcal{D}_1 = \{1, 7, 9, 11, 13, 15\}$. In the same way we proceed to subsequent orders $k = 3, 4, \dots$. In the FPU- β one follows the same steps, but for $r(k) = 2k + 1$.

iii) *Excitation representing a low-frequency packet of seed modes:* Let us consider as an initial excitation the packet of modes $\mathcal{D}_0 = \{1, 2, 3, 4\}$ for N large. Following the same procedure as above, in the FPU- α we find the sequence of excitations $\mathcal{D}_1 = \{5, 6, 7, 8\}$, $\mathcal{D}_2 = \{9, 10, 11, 12\}$, etc. We notice that at each order modes are excited *in groups*. In the same way, the β model yields $\mathcal{D}_1 = \{5, \dots, 12\}$, $\mathcal{D}_2 = \{13, \dots, 20\}$, etc.

These propagation rules can be generalized for s -dimensional q -tori corresponding to low-frequency packets of modes. The seed mode excitation $\mathcal{D}_0 = \{1, 2, \dots, s\}$ generates $\mathcal{D}_k = \{ks + 1, \dots, (k+1)s\}$ in the FPU- α , and $\mathcal{D}_k = \{(2k-1)s + 1, \dots, (2k+1)s\}$ in the FPU- β , with $k \geq 1$. Furthermore, we observe that $\mathcal{D}_k^\beta = \mathcal{D}_{2k-1}^\alpha \cup \mathcal{D}_{2k}^\alpha$. As shown in the next subsection, these rules imply that the resulting q -tori solutions exhibit *exponential energy localization profiles*.

iv) *Excitation representing a high-frequency packet of seed modes:* As an example, let us consider $\mathcal{D}_0 = \{28, 29, 30, 31\}$ in the $N = 32$ dimensional chain. In the FPU- α we find $\mathcal{D}_1 = \{1, \dots, 8\}$, then $\mathcal{D}_2 = \{20, \dots, 27\}$, etc. The general rule, by setting the last s modes $\mathcal{D}_0 = \{N - s, \dots, N - 1\}$ as seed modes, is: $\mathcal{D}_k = \{(k-1)s + 1, \dots, (k+1)s\}$, if $k = 2n + 1$ and $\mathcal{D}_k = \{N - (k+1)s, \dots, N - (k-1)s - 1\}$, if $k = 2n$. By the same way, in the FPU- β we find $\mathcal{D}_k = \{N - (k+1)s, \dots, N - (k-1)s - 1\}$, $\forall k$. Comparing the two models, we see that $\mathcal{D}_k^\beta = \mathcal{D}_{2k}^\alpha$.

v) *Discrete symmetry solutions:* Suppose $\mathcal{D}_0 = \{N/2\}$, or $\mathcal{D}_0 = \{2N/3\}$. We then find $\mathcal{D}_k = \mathcal{D}_0$ for all $k = 1, 2, \dots$ in both models, while in FPU- β the condition $\mathcal{D}_k = \mathcal{D}_0$ holds also for $\mathcal{D}_0 = \{N/3\}$. The q -breather solutions for these cases correspond to the ‘nonlinear normal modes’ of the FPU system [2, 27, 29], that coincide with the FPU-trajectories resulting from the same seed mode.

We note finally, that for q -breathers we have a general relation connecting the sequences of excitations \mathcal{D}_k in the α and in the β model, starting from the same seed mode. Namely, from Eq.(16) we find that $\mathcal{D}_k^\beta = \mathcal{D}_{2k}^\alpha$. In words, the mode excited at the k -th order in the FPU- β is the same as the mode excited at the $2k$ -th order in the FPU- α . This relation holds also for excitations of small packets around $N/4$, $N/2$ and $3N/4$, but it does not hold in the case (iii) (low-frequency packets of modes). In fact, for an arbitrary excitation we have $M_{2k}^\alpha = M_k^\beta$, but we only have $\mathcal{D}_k^\beta = \mathcal{D}_{2k}^\alpha$ provided that $M_{2k-1}^\alpha \cap M_{2k}^\alpha = \emptyset$.

2.4 Leading order terms

We close this section by giving an expression for the leading order terms of the solution $Q_q(t)$, $q \in \mathcal{D}_k$ (see Definition 1). This will be used in section 3 in order to predict the forms of energy localization profiles of q -tori.

Let $\mathcal{D}_0 = \{q_1, q_2, \dots, q_s\}$ be a 0-th order excitation set, $n^{(r)} \in \mathcal{D}_0^r$ an r -vector in \mathcal{D}_0^r and $\omega_n^{(r)} \equiv \{\omega_{n_1}, \dots, \omega_{n_r}\}$, $\phi_n^{(r)} \equiv (\phi_{n_1}, \dots, \phi_{n_r})$ its associated frequency and phase vectors respectively. Some basic features of the PL construction arising in accordance with the Definitions 1 – 4 of subsection 2.3 are:

i) If $q \in \mathcal{D}_k$, then $Q_q^{(k)}(t)$ is a leading order term of the series (8).

ii) The only modes that admit frequency corrections are those in \mathcal{D}_0 , for the rest holds $\omega_q = \Omega_q$, $q \notin \mathcal{D}_0$.

iii) At the k -th order, the expressions for $Q_q^{(k)}(t)$ contain divisors which are the products of k factors of the form $\Omega_q^2 - (\sigma^{(r(m))}\omega_n^{(r(m))})^2$, $m \leq k$. Since all frequencies are fixed in advance to incommensurable values, such divisors, albeit possibly quite small, can never become equal to zero exactly.

We determine the solutions of Eqs.(11) and (12), for the leading order terms $Q_q^{(k)}(t)$, starting by the 0-th order solution $Q_q^{(0)}(t)$ of Eq. (9). For convenience, in subsequent formulae we use exponential rather than trigonometric expressions. In both the α and β models, for $q \in \mathcal{D}_k$ we find (see 4)

$$Q_q^{(k)}(t) = \sum_{\substack{n^{(r)} \in \mathcal{D}_0^r \\ \sigma^{(r)} \in \Sigma^r}} \mathcal{R}_q^{(k)}(n^{(r)}) \mathcal{K}_q^{(k)}(n^{(r)}) e^{i\sigma^{(r)}(\omega_n^{(r)}t + \phi_n^{(r)})} \quad (17)$$

where $r(k) = k + 1$ for the FPU- α and $r(k) = 2k + 1$ for the FPU- β . In the above expression, the factor $\mathcal{R}_q^{(k)}$ is given by

$$\mathcal{R}_q^{(k)}(n^{(r)}) = \frac{(-1)^k}{2^r} \cdot \frac{\Omega_q \Omega_{n_1} \dots \Omega_{n_r} A_{n_1} \dots A_{n_r}}{\Omega_q^2 - (\sigma^{(r)}\omega_n^{(r)})^2} \quad (18)$$

and $\mathcal{K}_q^{(k)}$ by the recursive relation

$$\mathcal{K}_{q;\alpha}^{(k)}(n^{(r)}) = \sum_{\substack{l_1, l_2=0 \\ l_1+l_2=k-1}}^{k-1} \sum_{\substack{m_i \in \mathcal{D}_{l_i} \\ i=1,2}} \mathfrak{L}_{m_1}^{(l_1)}(n^{(r(l_1))}) \mathfrak{L}_{m_2}^{(l_2)}(n^{(r(l_2))}) \mathcal{K}_{m_1}^{(l_1)}(n^{(r(l_1))}) \mathcal{K}_{m_2}^{(l_2)}(n^{(r(l_2))}) B_{qm_1 m_2} \quad (19)$$

with

$$n^{(r(k))} = \underbrace{(n_1, \dots, n_{r(l_1)})}_{n^{(r(l_1))}} \underbrace{(n_{r(l_1)+1}, \dots, n_{r(k)})}_{n^{(r(l_2))}}$$

in the α case and

$$\begin{aligned} \mathcal{K}_{q;\beta}^{(k)}(n^{(r)}) = & \sum_{\substack{l_1, l_2, l_3=0 \\ l_1+l_2+l_3=k-1}}^{k-1} \sum_{\substack{m_i \in \mathcal{D}_{l_i} \\ i=1,2,3}} \mathfrak{L}_{m_1}^{(l_1)}(n^{(r(l_1))}) \mathfrak{L}_{m_2}^{(l_2)}(n^{(r(l_2))}) \mathfrak{L}_{m_3}^{(l_3)}(n^{(r(l_3))}) \\ & \mathcal{K}_{m_1}^{(l_1)}(n^{(r(l_1))}) \mathcal{K}_{m_2}^{(l_2)}(n^{(r(l_2))}) \mathcal{K}_{m_3}^{(l_3)}(n^{(r(l_3))}) C_{qm_1 m_2 m_3} \quad , \end{aligned} \quad (20)$$

with

$$n^{(r(k))} = \underbrace{(n_1, \dots, n_{r(l_1)})}_{n^{(r(l_1))}} \underbrace{(n_{r(l_1)+1}, \dots, n_{r(l_1)+r(l_2)})}_{n^{(r(l_2))}} \underbrace{(n_{r(l_1)+r(l_2)+1}, \dots, n_{r(k)})}_{n^{(r(l_3))}}$$

in the β case, setting, in both cases, $\mathcal{K}_q^{(0)} = 1$ at $k = 0$. The terms $\mathfrak{L}_m^{(l)}$, $m \in \mathcal{D}_l$ entering the expressions (19) and (20) are

$$\mathfrak{L}_m^{(l)}(n^{(r(l))}) = \frac{\Omega_m^2}{\Omega_m^2 - (\sigma^{(r(l))}\omega_n^{(r(l))})^2} \quad (21)$$

for $k > 0$, or $\mathfrak{L}_q^{(0)} = 1$ at $k = 0$. Both quantities $\mathcal{K}_{q;\alpha}^{(k)}$, and $\mathcal{K}_{q;\beta}^{(k)}$ are polynomials of degree $k - 1$ in the terms $\mathfrak{L}_m^{(l)}$, $l = 0, 1, \dots$ and can be computed iteratively. Explicit expressions for the first few orders of the mapping (19) are given in 4.

3 Numerical examples. Localization profiles

In this section we provide various numerical tests on the dynamics of the q -tori and their neighboring FPU-trajectories. In these, we compare computer-algebraic series calculations with purely numerical calculations. In particular, we examine and correlate the energy spectra in both cases. Furthermore, we derive the form of the localization spectra for particular q -tori solutions and check up to what extent various features predicted by theory appear in the localization spectra of the numerically integrated orbits. In 4 we give a table with the frequencies and amplitudes used throughout all the examples below, in order to allow for reproducibility of the results.

3.1 A q -torus example

As explained in subsection 2.2, in numerical computations we work with finite truncations of both series (8) and (10). Furthermore, for a specific choice of frequencies ω_{q_i} we solve numerically the truncated Eqs.(10) in order to specify the corresponding numerical values of the amplitudes A_{q_i} . Then, we substitute A_{q_i} into the series (8) truncated at the order k_0 .

In the sequel, we denote by

$$Q_q^{PL,k_0}(t) = Q_q^{(0)}(t) + \mu Q_q^{(1)}(t) + \dots + \mu^{k_0} Q_q^{(k_0)}(t)$$

$q = 1, \dots, N - 1$ the approximate solutions of $Q_q(t)$ obtained by the above procedure. By differentiating with respect to time, we also specify a truncated series for the canonical momenta $P_q^{PL,k_0}(t) = \dot{Q}_q^{PL,k_0}(t)$. Having both expressions at hand, we specify *initial conditions* $Q_q^{PL,k_0}(0)$ and $P_q^{PL,k_0}(0)$ which, in this approximation, should lead to motion on a torus with the prescribed frequencies. To verify the above statement, we integrate numerically the orbits³ resulting from such initial conditions and obtain $Q_q^{PLn,k_0}(t)$, $P_q^{PLn,k_0}(t)$, in order to make various comparison tests between the PL and their numerical realization (PLn). A main comparison refers to the *normalized averaged energy spectra* in a time interval $2T/3 \leq t \leq T$. We define the average harmonic energy of the q -th mode as

$$\overline{E}_q(T) = \frac{3}{T} \int_{2T/3}^T E_q(t) dt \quad (22)$$

where E_q is given by Eq.(5). By introducing the re-scaled wavenumber $\kappa = q/N$, we plot the normalized averaged energy spectrum $e_\kappa = \overline{E}_q/E$ versus κ , where E is the total energy given to the system. Such plots allow us to compare the averaged energy spectra e_κ^{PL,k_0} , e_κ^{PLn,k_0} , and also the spectra e_κ of FPU-trajectories, for various solutions corresponding to N fixed, but also N varied, which is a case of interest in the solutions arising from so-called ‘extensive’ sets of initial conditions (see below).

As a first example, we consider a 4-torus solution in the $FPU - \alpha$ model with $N = 32$, $\alpha = 0.33$, when the initial excitation refers to the first four lowest frequency modes, i.e. $\mathcal{D}_0 = \{1, 2, 3, 4\}$, with the chosen frequencies given in the first group of the table in 4. The truncation order is $k_0 = 11$ and all phases are set as $\phi_{q_i} = 0$. Solving numerically Eqs.(10) we specify the amplitudes A_1, A_2, A_3, A_4 (see 4), which result to $E = 0.000182466$.

³by a 4-th order symplectic kinetic-potential splitting algorithm

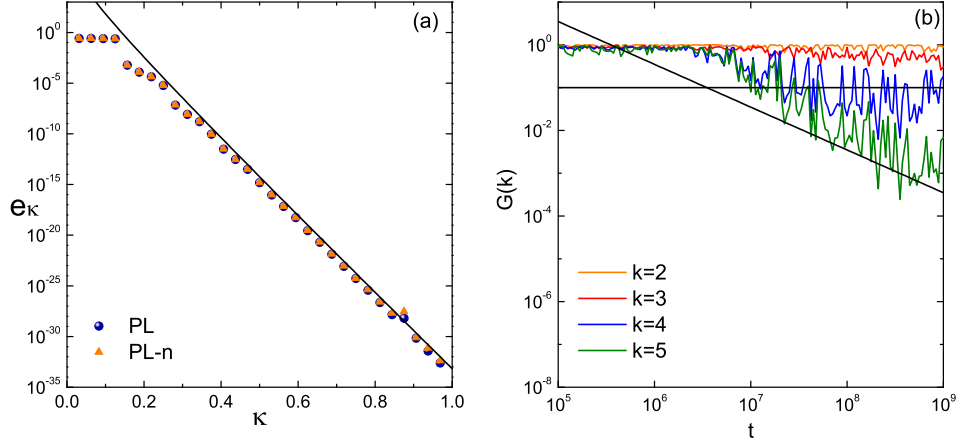


Figure 1: (a) Normalized averaged exponential spectra e_κ versus $\kappa = q/N$ for the system with $\mathcal{D}_0 = \{1, 2, 3, 4\}$, $\alpha = 0.33$, $E = 0.000182466$, $N = 32$, for a total time $T = 10^6$. The blue spheres correspond to a q -torus construction with the truncated PL series, denoted $Q_q^{PL,11}(t)$. The orange triangles correspond to a numerical solution, denoted $Q_q^{PLn,11}(t)$, obtained by numerically integrating the FPU equations of motion with initial conditions $Q_q^{PL,11}(0)$, $P_q^{PL,11}(0)$. The continuous line is $\log(e_\kappa) = 3.49545 - 36.6613\kappa - 2 \log(\kappa)$. (b) GALI indices (see text) for $k = 2, 3, 4, 5$ calculated for the orbit of the orange spectrum in (a).

Fig.1(a) shows a comparison of the normalized averaged spectra e_κ^{PL} (blue) and e_κ^{PLn} (orange) at integration time $T = 10^6$. The continuous line is obtained by the method described in subsection 3.2 below, which yields a prediction for the mean exponential slope of the energy localization profile based on the leading order terms of Eq.(17) for an initial excitation corresponding to the first s lower frequency modes.

Since we only compute the numerical coefficients of the truncated PL series solution, we have no rigorous demonstration of the convergence of the series. In [11] we will discuss several criteria examining this question. Here, instead, we rely, as in [10], in the use of the Generalized Alignment Index (GALI) method [23, 24, 25], which is a numerical method allowing us to determine the dimension of a stable torus by the temporal behavior of a set of indicators (G_2, G_3, \dots) computed via an integration of the variational equations of motion along with the original ones. Fig.1(b) shows in double logarithmic scale the evolution of GALI indices for $k = 2, 3, 4, 5$. The indices G_k for $k = 2, 3$ converge very fast to a constant value, while G_4 oscillates around its average value after an initial decay lasting for a rather long time, $t = 3 \cdot 10^7$. On the other hand, at times greater than the time of stabilization of G_4 , the index G_5 clearly decays as $1/t$, up to at least the time 10^9 . Following [24, 25], we conclude that the numerical orbit $Q_q^{PLn,11}(t), P_q^{PLn,11}(t)$ lies on a torus of dimension $s = 4$. In fact, since we only have a finite precision in the initial conditions, a more precise statement, is that the orbit follows a q -torus dynamics for times up to 10^9 , so that no large scale chaotic diffusion phenomena can occur for this orbit within this timescale.

3.1.1 Comparison with an FPU-trajectory. Stages of dynamics

FPU-trajectories with initial conditions close to q -tori appear to exhibit, on the average, similar localization phenomena as the q -tori for quite long integration times. However, as in [22], we also find that the FPU-trajectories undergo some well distinct ‘stages of dynamics’ that further characterize the time evolution of their average normalized energy spectra.

As an example, we consider the FPU-trajectory with initial conditions $Q_q(0) = A_q$, for $q = 1, 2, 3, 4$,

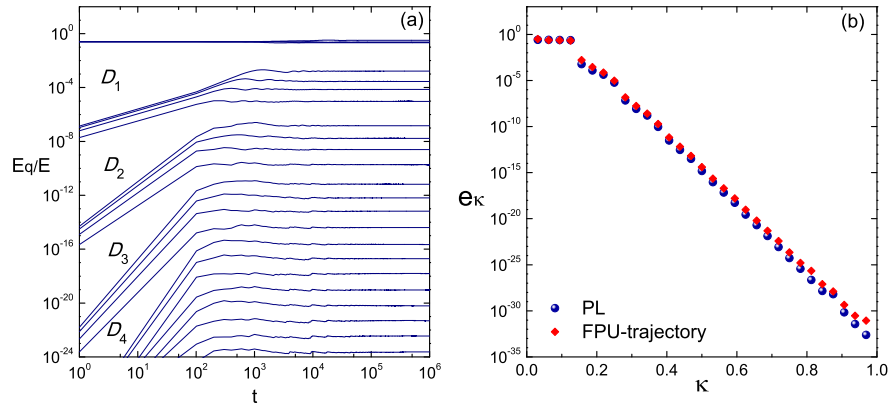


Figure 2: (a) Time evolution of the normalized averaged energies $\overline{E}_q(t)/E$, in double logarithmic scale, for the FPU-trajectory arising from the excitation of the first $s = 4$ modes with initial conditions $Q_q(0) = A_q$ if $q = 1, 2, 3, 4$ and $Q_q(0) = 0$ else, and system's parameters as in Fig.1 for the q -torus solution. (b) Comparison of the normalized averaged energy spectra e_κ versus κ of the q -torus solution of Fig.1 (blue) and the corresponding FPU-trajectory (orange) over a total integration time $T = 10^6$.

and $Q_q(0) = 0$, for $q = 5, \dots, 31$, $P_q(0) = 0$, $q = 1, \dots, 31$ in the FPU- α system with the same parameters of the q -torus solution of Fig.1. The initial distance in phase space between the FPU and the q -torus trajectories is of order $O(\mu)$, where in this case $\mu \approx 4 \times 10^{-2}$.

Fig.2(a) shows the evolution of the normalized averaged energies $\overline{E}_q(T)/E$ for all the modes $q = 1, \dots, N - 1$ of the above FPU-trajectory. We observe that the modes $q = 1, 2, 3, 4$, which shared exclusively the total energy at $T = 0$, continue to share most of the energy at all subsequent times T . As a result, $\overline{E}_q(T)/E$ remains practically constant for these 4 modes, exhibiting only small variations (of order 10^{-4}) which correspond to the energy gradually transferred to the remaining modes. Such variations are unobservable on the scale of Fig.2 in the corresponding curves for the modes $q = 1, 2, 3, 4$.

However, the energy transfer is observable by plotting the time evolution of $\overline{E}_q(T)/E$ for all other modes. In fact, we observe that this transfer takes place in a rather short time interval, of order $T = 10^3$ for the modes $q = 5, 6, 7, 8$, and $T = 10^2$ for the remaining modes. Following the terminology introduced in [22], this phenomenon corresponds to the so-called *first stage* of dynamics in the FPU- α system. In [22] it was stressed that the transfer of energy during this stage appears to be a phenomenon explained by regular ('integrable-like') dynamics, since a similar phenomenon is observed in the Toda lattice, which is an integrable system. Furthermore, the energy growth during the first stage of dynamics is characterized by a power law growth with respect to time, a process called 'secular avalanche'.

It is important to point out that, also here in the case of FPU-trajectories, the modes form well distinguished groups. These groups correspond exactly to the groups \mathcal{D}_k of the sequence of excitations generated by the q -torus solution of Fig.1 with initial excitation $\mathcal{D}_0 = \{1, 2, 3, 4\}$, namely we have: $\mathcal{D}_1 = \{5, 6, 7, 8\}$, $\mathcal{D}_2 = \{9, 10, 11, 12\}$, ..., or, in general, $\mathcal{D}_k = \{ks + 1, \dots, (k + 1)s\}$. It is observed that, during this secular avalanche process, for all modes $q \notin \mathcal{D}_0$ in the same group \mathcal{D}_k the quantity \overline{E}_q/E grows in time by almost the same power-law, i.e. the energy spectra behave as $\overline{E}_q(t)/E \sim t^{c_q(k)}$, where the exponent is almost constant within a group: $c_q(k) = c(k) + \epsilon_q$, with $|\epsilon_q| \ll 1$ for all $q \in \mathcal{D}_k$.

On the other hand, at the end of the first stage of dynamics the normalized averaged energy spectrum for the FPU-trajectory appears to be stabilized to a form persisting at least up to the end of the numerical integration, at $T = 10^6$. This stabilized spectrum displays an exponential profile, which is strikingly similar to the q -torus profile shown in Fig.1(a), as can be seen by a direct superposition of the two spectra

(Fig.2(b)). In particular, we observe that the modes in the spectrum of the FPU-trajectory, during this metastable state, remain separated in the same groups, exactly as in the q -torus solution.

We emphasize that this effect cannot be considered as a trivial consequence of the proposition of subsection 2.3, since the latter only concerns a formal aspect of the PL series construction for q -tori, while the separation of the modes in the case of the FPU-trajectory is a *dynamical* phenomenon, characterizing the energy transfer process. The fact that, the final groups defined in either case are the same, indicates some deeper connection between q -torus and FPU-trajectory solutions. However, although the FPU-trajectories appear to follow effectively a q -torus dynamics up to a long time, contrary to q -tori, most FPU-trajectories enter eventually into the stage of approach to energy equipartition (the so-called ‘second stage of dynamics’ in [22]).

3.2 q -Tori low frequency packet solutions and exponential energy localization

The q -torus as well as the FPU-trajectory examined in the previous subsection are examples of a class of solutions of particular interest in the literature (see [14, 15, 17, 18, 19]), namely solutions corresponding to the initial excitation of a *packet* of low-frequency modes. In fact, it is numerically found that, for values of the specific energy beyond some threshold, low-frequency packets of modes are formed naturally, even if initially is excited only *one*, e.g. the $q = 1$ mode. Some questions of central interest in the literature concern the dependence of: i) the width of natural packets ii) the exponential slope of the energy spectrum of the remaining modes, on system’s parameters E , N etc (see [16] for a review).

In the sequel we examine the form of localization profiles for q -torus solutions associated with an initial excitation of a low-frequency packet of modes. We obtain theoretical results based on a leading order term analysis of the PL series for q -tori of subsection 2.4. Furthermore, we compare these results with ones found numerically for FPU-trajectories with a similar initial excitation.

Our main result for the FPU- α can be stated as follows: in subsection 2.3 it was mentioned that, for q -tori, an initial excitation $\mathcal{D}_0 = \{1, 2, \dots, s\}$ in the PL series leads to the sequence of mode excitations $\mathcal{D}_k = \{ks + 1, \dots, (k + 1)s\}$. Starting, now, from the median mode in the group \mathcal{D}_k , i.e. the mode $q_{mid} = ks + [s/2]$, we can obtain estimates of the size of the leading term $Q_{q_{mid}}^{(k)}$ given by Eq.(17) and derive estimates on the magnitude of the harmonic energy $E_{q_{mid}}^{(k)}$, which is hereafter denoted by $E^{(k)}$. Then, we have:

$$E^{(k)} \sim \frac{(k + 1/2)^2 \varepsilon}{M} \left(\frac{\alpha^2 N^4 \varepsilon}{\pi^4 s^4} \right)^k \quad (23)$$

where $M = s/N$ is the fraction of initially excited modes with respect to the total number of modes. The derivation of Eq. (23) is given in 4.

Normalizing Eq.(23) we obtain

$$\log e_\kappa \sim \frac{\log \lambda}{M} \kappa + 2 \log \kappa - \log(\lambda^{1/2} M^3 N) \quad (24)$$

where $\lambda = \alpha^2 \varepsilon / \pi^4 M^4$. The main prediction is that if α, ε , and the fraction $M = s/N$ are kept fixed, *the normalized energy profiles of q -tori remain unaltered as N increases.*

This prediction becomes hardly possible to test by a direct construction of the q -tori solutions via PL series, because as N increases, we quite soon encounter the limits of computer memory required for storing the coefficients produced by the computer-algebraic program. However, taking into account the evidence presented in subsection 3.1.1, that FPU-trajectories with the same initial excitations as q -tori exhibit similar localization profiles, we can test numerically the extent up to which the invariance of the normalized averaged energy spectrum holds for FPU-trajectories as well.

Such a test is made in Fig.3. In (a) we give the normalized averaged energy spectrum e_κ as a function of the re-scaled wavenumber $\kappa = q/N$ for an FPU-trajectory with $\alpha = 0.33$, $M = 1/8$, and $\varepsilon = 1.5625 \times 10^{-8}$.

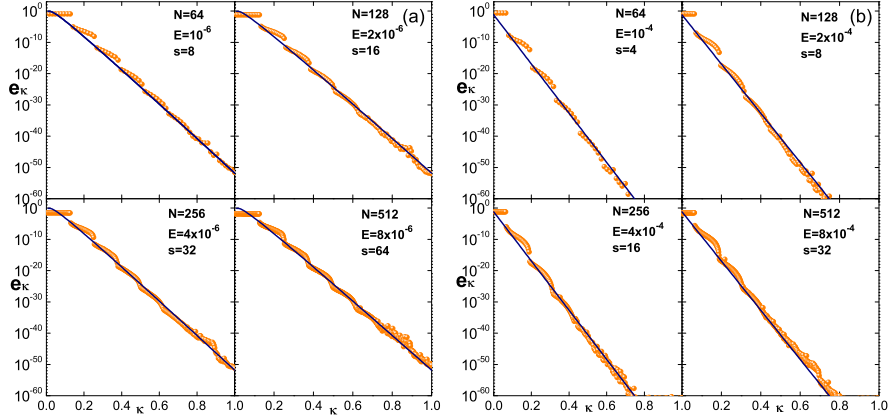


Figure 3: Normalized averaged energy spectra e_κ versus κ for FPU-trajectories (orange spheres) in both the FPU- α and FPU- β models, keeping the specific energy ε and the ratio of initially excited modes M fixed. The parameters are: (a) FPU- α model with $\alpha = 0.33$, $M = 1/8$, $\varepsilon = 1.5625 \times 10^{-8}$. (b) FPU- β model with $\beta = 0.3$, $M = 1/16$ and $\varepsilon = 1.5625 \times 10^{-6}$. In (a), the blue line in all panels corresponds to the theoretical prediction of Eq.(24) based on the leading order term analysis for q -tori. This is given by $\log e_\kappa = -56.27\kappa + 4.46 + 2 \log \kappa$. In (b) the blue line corresponds to a similar prediction for the FPU- β , given by Eq.(26). We find $\log e_\kappa = -78.64\kappa - 1.204$.

We computed these trajectories by progressively increasing N , namely $N = 64, 128, 256$ and 512 . The energy spectra of Fig.3 are all evaluated at $T = 10^6$. The solid line corresponds to the fitting law of Eq. (24), which, for the adopted parameters, takes the form indicated in the figure caption. The main remark is that *the same* line fits all re-scaled normalized spectra, for different N (while the fraction of initially excited modes $M = 1/8$ as well as the specific energy $\varepsilon = 1.5625 \times 10^{-8}$ are kept constant).

A question of central interest regards the upper limit in the specific energy for which the normalized spectra for the FPU-trajectories continue to exhibit exponential localization. Eq.(23) allows us to obtain an upper limit, by requiring that $\lambda = \alpha^2 \varepsilon / \pi^4 M^4 < 1$. However, as we approach the upper limit $\varepsilon = \pi^4 M^4 / \alpha^2$, the analysis based on only the leading order terms of the PL series ceases to be valid, since important contributions to the energy spectrum are made also by the higher order terms in each mode's series expansion of Eq.(8).

The condition $\lambda < 1$ implies $s > \alpha^{1/2} \varepsilon^{1/4} N$. Thus Eq.(23) applies when the initially excited packet has a width larger than the width of the so-called natural packets [14, 17, 18, 19]. In the case of natural packets, it is found that by the excitation of a number of low frequency modes satisfying $s < \alpha^{1/2} \varepsilon^{1/4} N$, the so resulting energy spectrum exhibits a plateau of width $\alpha^{1/2} \varepsilon^{1/4} N$ (larger than the initially excited modes). Furthermore, there is evidence that the slope $\tilde{\sigma}$ of the exponential energy localization profile $e_\kappa \sim \exp(-\tilde{\sigma} \cdot \kappa)$ depends linearly on $\alpha^{-1/2} \varepsilon^{-1/4}$ [20]. This is in contrast to the slope which refers to q -tori solutions of Eq.(23), that depends logarithmically on $[\alpha^{-1/2} \varepsilon^{-1/4}]^{-4}$ and points out that different choices in the fraction of the initially excited low-frequency modes result in different exponential laws.

q -Tori for low-frequency packets in the FPU- β For the sake of completeness we report the results of our previous work [10], concerning exponential energy localization in the FPU- β model. Assuming the initial excitation to be $\mathcal{D}_0 = \{1, 2, \dots, s\}$, the sequence of mode excitations in the PL series at the orders $k = 1, 2, \dots$ is $\mathcal{D}_k = \{(2k-1)s+1, \dots, (2k+1)s\}$. Estimating the size of the median mode $q_{mid,k} = 2ks$ in each group \mathcal{D}_k via Eq.(17), we are lead to an estimate for the energy spectra of q -tori with the above

excitation, namely

$$E^{(k)} \simeq \frac{\varepsilon}{M} \left(\frac{\beta^2 \varepsilon^2}{\pi^4 M^4} \right)^k \quad (25)$$

where $M = s/N$. Using re-scaled variables as in the α case, Eq.(25) takes the form

$$\log e_\kappa \simeq \frac{\log \lambda}{M} \kappa - \log s \quad (26)$$

where $\lambda = \beta\varepsilon/\pi^2 M^2$. We find a similar result as in the α case, namely Eq.(26) implies that by keeping both the specific energy ε and the fraction of excited modes M fixed, while N increases, the normalized exponential profile remains invariant. Again, in order that the analysis be valid, one must have $s > N(\beta\varepsilon)^{1/2}$, implying that the initial excitation should be in a regime quite different from that of natural packets. In fact, in the present case as well, Eq.(26) describes correctly the localization profile provided that $\lambda \ll 1$ (see also [10]).

As a numerical test of the above predictions we use again numerical computations based on FPU-trajectories rather than exact q -tori solutions. The four panels of Fig.3(b) show the normalized averaged spectra e_κ of FPU-trajectories, along with the predictions of Eq.(26), for the fixed values $M = s/N = 1/16$, and $\varepsilon = 1.5625 \cdot 10^{-6}$. We observe again that the spectrum remains practically invariant with increasing N .

3.3 Localization patterns for arbitrary initial excitations

So far, we focused on q -tori, and their neighboring FPU-trajectories corresponding to initial excitations in the low-frequency part of the spectrum. However, it is possible to see that energy localization appears also in cases where the initial excitation has quite different features than in the case of packets of low-frequency modes. In particular, we will examine now q -tori solutions in the FPU- α system produced by an initial excitation \mathcal{D}_0 consisting of a small set of s modes *arbitrarily distributed* in q -space. We give several such examples, in which we vary s , N , E , as well as \mathcal{D}_0 . As in the previous example of Fig.1, in all present cases we compare the normalized averaged energy spectra e_κ^{PL} obtained with the PL series, with the ones e_κ^{PLn} obtained by numerical integration of the equations of motion for the initial conditions $Q_q^{PL}(0)$, $P_q^{PL}(0)$, $q = 1, \dots, N-1$.

Example 1: evenly distributed initial excitation. In the FPU- α with $N = 32$, we construct a q -torus starting from the 0-th order excitation $\mathcal{D}_0 = \{1, 11, 21, 31\}$, when the frequency values for $\omega_1, \omega_{11}, \omega_{21}, \omega_{31}$ are chosen as in the second group of 4. The truncation order here is $k_0 = 11$. Solving numerically Eqs.(10) we specify the values of the amplitudes A_1, A_{11}, A_{21} and A_{31} . The total energy is $E = 0.001563$.

Fig.4(a) shows the normalized averaged energy spectrum for the above q -torus solution. Energy localization is manifestly present, since we observe the formation of four peaks of the energy spectrum around the seed modes 1,11,21 and 31. The localization pattern is readily understood by computing the sequence of mode excitations \mathcal{D}_k deduced by the proposition of subsection 2.3. Namely, we find $\mathcal{D}_1 = \{2, 10, 12, 20, 22, 30\}$, $\mathcal{D}_2 = \{3, 9, 13, 19, 23, 29\}$, $\mathcal{D}_3 = \{4, 8, 14, 18, 24, 28\}$, $\mathcal{D}_4 = \{5, 7, 15, 17, 25, 27\}$ etc. We observe that consecutive modes, adjacent (on either side) to the initially excited ones, are excited at subsequent orders of perturbation theory. Thus, starting for example from the mode $q = 11$, the modes $q = 10, 12$ are excited at first order, $q = 9, 13$ at second order, etc. This explains the formation of the peaks in the spectrum. In fact, the pairs $\{10, 12\}$, $\{9, 13\}$, etc. share quite similar energies, corresponding to excitation amplitudes $O(\mu)$, $O(\mu^2)$, ... As a result, the local form of the energy spectrum on either side of one peak is exponential.

Finally, as evident in Fig.4(a), we find a very precise agreement between the normalized spectrum corresponding to the analytical solution E_q^{PL} , and the one E_q^{PLn} obtained by numerical integration of the

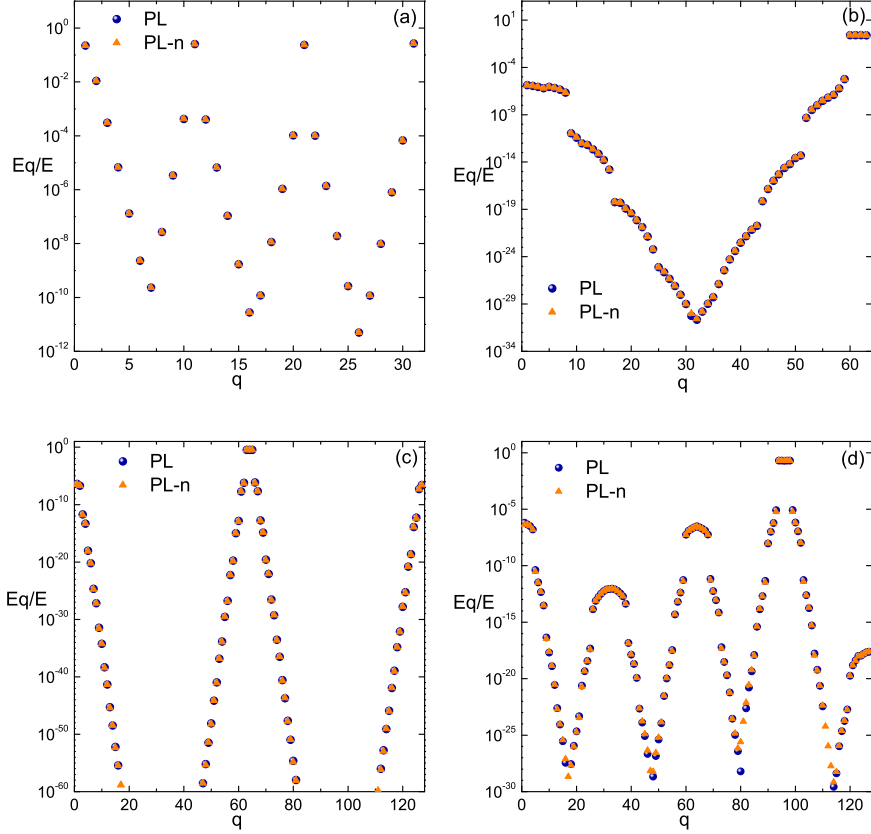


Figure 4: Normalized averaged energy spectra E_q versus q , deduced by the PL series q -torus solution (blue spheres), or by a numerical integration (PLn) with initial conditions on a q -torus (orange triangles, see text). (a) $N = 32$, $\alpha = 0.33$, $\mathcal{D}_0 = \{1, 11, 21, 31\}$, (b) $N = 64$, $\alpha = 1$ with $\mathcal{D}_0 = \{60, 61, 62, 63\}$. (c) $N = 128$, $\alpha = 1$ with $\mathcal{D}_0 = \{63, 64, 65\}$. (d) $N = 128$, $\alpha = 1$ and $\mathcal{D}_0 = \{94, 95, 96, 97, 98\}$. The chosen frequency values, and resulting amplitudes and energies in each case are given in 4.

initial conditions on the q -torus. This fact indicates that at the truncation order $k_0 = 11$ the solution has converged to a good accuracy.

Example 2: initial excitation in the high-frequency part of the spectrum. We consider a q -torus solution found by PL series in the case $N = 64$, $\alpha = 1$, when $\mathcal{D}_0 = \{60, 61, 62, 63\}$, while the choice in the frequencies and the resulting amplitudes are shown in the third group of 4. The truncation order of the series is $k_0 = 8$ and the energy is $E = 0.000883$.

Fig.4(b) shows the resulting normalized averaged energy spectrum for the above q -torus solution. This displays several features similar to the case of a low-frequency excitation. Namely, we observe the formation of groups of consecutive modes sharing a similar amount of energy. The sequence of mode excitations in this case turns out to be $\mathcal{D}_1 = \{1, \dots, 8\}$, $\mathcal{D}_2 = \{52, \dots, 59\}$, $\mathcal{D}_3 = \{9, \dots, 16\}$, $\mathcal{D}_4 = \{44, \dots, 51\}$, etc.

Finally, we note again the exponential fall of the energy along two separate branches of the spectrum, namely a low-frequency and a high-frequency branch.

Example 3: excitation in the middle part of the spectrum. We consider the middle modes initial excitation $\mathcal{D}_0 = \{63, 64, 65\}$ in the FPU- α with $\alpha = 1$, $N = 128$, and with frequencies and amplitudes displayed in the fourth group of 4. The PL series are truncated at $k_0 = 16$ and the energy of the system is $E = 7.63469 \times 10^{-5}$.

In the corresponding normalized averaged energy spectra E_q^{PL}/E and E_q^{PLn}/E (Fig.4(c)) we observe that three energy peaks are formed: by the lowest, the highest and the middle modes of the spectrum. We find that the sequence of mode excitations here is $\mathcal{D}_1 = \{1, 2, 126, 127\}$, $\mathcal{D}_2 = \{61, 62, 66, 67\}$, $\mathcal{D}_3 = \{3, 4, 124, 125\}$, $\mathcal{D}_4 = \{59, 60, 68, 69\}$, etc.

Example 4: excitation in the 3/4 part of the spectrum. We consider, as before, $N = 128$, $\alpha = 1$, and an initial excitation $\mathcal{D}_0 = \{94, 95, 96, 97, 98\}$. The chosen frequency values and the so-resulting amplitudes are shown in the fifth group of 4. The truncation order is $k_0 = 9$ and the energy is $E = 0.000649478$.

At subsequent orders, we now find the sequence of mode excitations $\mathcal{D}_1 = \{1, 2, 3, 4\} \cup \{60, \dots, 68\}$, $\mathcal{D}_2 = \{26, \dots, 38\} \cup \{90, \dots, 93\} \cup \{99, \dots, 102\}$, $\mathcal{D}_3 = \{5, \dots, 8\} \cup \{56, \dots, 72\} \cup \{120, \dots, 127\}$, $\mathcal{D}_4 = \{22, \dots, 25\} \cup \{39, \dots, 42\} \cup \{86, \dots, 89\} \cup \{103, \dots, 106\}$, etc. This leads to the localization pattern shown in Fig.4(d).

Generalization: We now generalize results on the localization patterns formed by initial excitations of packets, around the locations in q -space corresponding the one fourth, half and three thirds of the spectrum. We suppose that each packet is of the form $\mathcal{D}_0 = [\kappa_0 - \epsilon, \kappa_0 + \epsilon]$, having a width equal to $s/N = 2\epsilon$, $\epsilon \ll 1$ in the normalized q -space $\kappa = q/N \in [0, 1]$. In order to specify the sequence of mode excitations \mathcal{D}_k at subsequent orders, we first specify the sets M_k defined in Eq.(14), whereby the sets \mathcal{D}_k are immediately derived by the relation $\mathcal{D}_k = M_k \setminus \cup_{0 \leq j \leq k-1} M_j$. Examining in detail the case of excitations around the re-scaled wavenumbers $\kappa_0 = 1/4, 1/2$, or $3/4$ we have:

1) For $\kappa_0 = 1/4$ we find $M^{(k)} = [0, \epsilon(k+1)] \cup [1/2 - \epsilon(k+1), 1/2 + \epsilon(k+1)] \cup [1 - \epsilon(k+1), 1]$, if $k = 2n + 1$, or $M^{(k)} = [1/4 - \epsilon(k+1), 1/4 + \epsilon(k+1)] \cup [3/4 - \epsilon(k+1), 3/4 + \epsilon(k+1)]$, if $k = 2n$. The resulting localization pattern displays three peaks around $\kappa = 0, 1/2$, and 1 , produced at odd orders, and two peaks around $1/4$ and $3/4$, produced at even orders. The total pattern is shown in Fig.5(a). In this figure, the ordinate in all panels indicates the order k of the PL series at which the corresponding mode, of wavenumber $\kappa = q/N$, is first excited. In fact, according to the leading order term analysis of the PL series discussed above we have $\log e_\kappa \sim \kappa$. Thus, the patterns shown in all panels of Fig.5 are similar to the normalized averaged energy spectra for the corresponding excitations when plotted in semi-logarithmic scale.

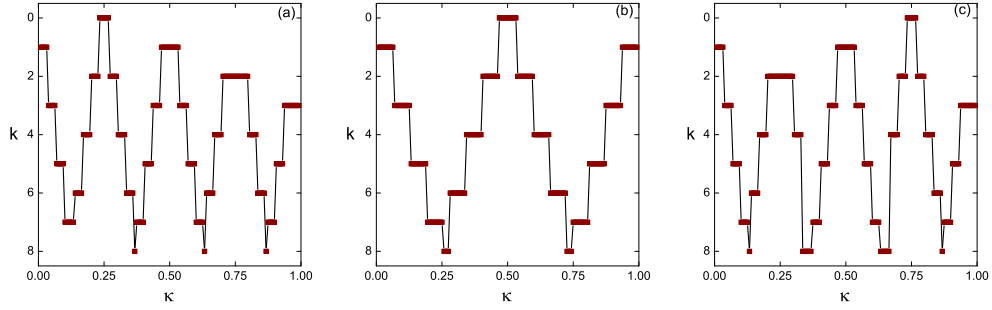


Figure 5: Propagation of modes for an initial excitation $\mathcal{D}_0 = [\kappa_0 - \epsilon, \kappa_0 + \epsilon]$ when (a) $\kappa_0 = 1/4$, (b) $\kappa_0 = 1/2$ and (c) $\kappa_0 = 3/4$. In all panels, the ordinate yields the order k of perturbation theory at which the mode q is first excited. Since in the exponential energy localization regime we always have $\log e_\kappa \sim \kappa$, the patterns shown in the present panels are similar to the energy spectra for the same excitations plotted in semi-logarithmic scale.

2) For $\kappa_0 = 1/2$ we find $M^{(k)} = [0, \epsilon(k+1)] \cup [1 - \epsilon(k+1), 1]$, if $k = 2n + 1$, or $M^{(k)} = [1/2 - \epsilon(k+1), 1/2 + \epsilon(k+1)]$, if $k = 2n$. Thus, we have two localization peaks around $\kappa = 0$ and $\kappa = 1$ created by contributions at odd orders of the PL series, and one more peak around $\kappa = 1/2$ for contributions at even orders. The overall localization pattern is shown in Fig.5(b).

3) For $\kappa_0 = 3/4$ we find similar results as in case (1), since $M^{(k)} = [0, \epsilon(k+1)] \cup [1/2 - \epsilon(k+1), 1/2 + \epsilon(k+1)] \cup [1 - \epsilon(k+1), 1]$, if $k = 2n + 1$ and $k > 1$, and $M^{(k)} = [1/4 - \epsilon(k+1), 1/4 + \epsilon(k+1)] \cup [3/4 - \epsilon(k+1), 3/4 + \epsilon(k+1)]$, if $k = 2n$. In fact, the only difference with respect to case (1) concerns the order $k = 1$, for which it turns out that $M^{(1)} = [0, 2\epsilon] \cup [1/2 - 2\epsilon, 1/2 + 2\epsilon]$. The resulting localization pattern is shown in Fig.5(c).

3.4 q -breathers and FPU-trajectories

The existence, stability, and energy localization properties of q -breathers have been studied extensively in [3]–[9]. For low energies, it is found that FPU-trajectories with an initial excitation of the same ‘seed mode’ and energy as stable q -breathers exhibit similar energy localization phenomena as the q -breathers for quite long integration times.

In the sequel we examine q -breathers as a particular case of one-dimensional q -tori constructed via PL series. At any fixed order k , the number of terms in the resulting series is substantially smaller for q -breathers than for q -tori of any other dimension $s > 1$. This fact allows us to construct the series up to a very high order (in the case $N = 32$ we were able to compute examples of PL series for q -breathers up to the truncation order $k_0 = 250$). Even so, for reasons explained in the accompanying paper [11], the convergence of the resulting series is very slow, and in practice we obtain little gain in precision after a truncation order near $k_0 = 50$. In most of our tried examples, the precision achieved for the computation of initial conditions on a q -breather using PL series is typically 4 to 6 significant digits, while in some cases we reach 10 (see below). However, we also use these numbers as an *initial guess* in order to determine more digits in the initial conditions via a root-finding technique. This is possible especially for q -breathers, which are periodic trajectories, while we cannot use such technique in the case of q -tori of dimension higher than one. Using the Newton-Raphson method, we specify initial conditions on q -breathers up to 12–14 significant digits.

As a first example, we consider the classical case where we excite initially the mode $q_0 = 1$ in the FPU- α . The sequence of mode excitations is $q_k = k + 1$. Fig.6 refers to a calculation for $N = 32$, $\alpha = 0.33$

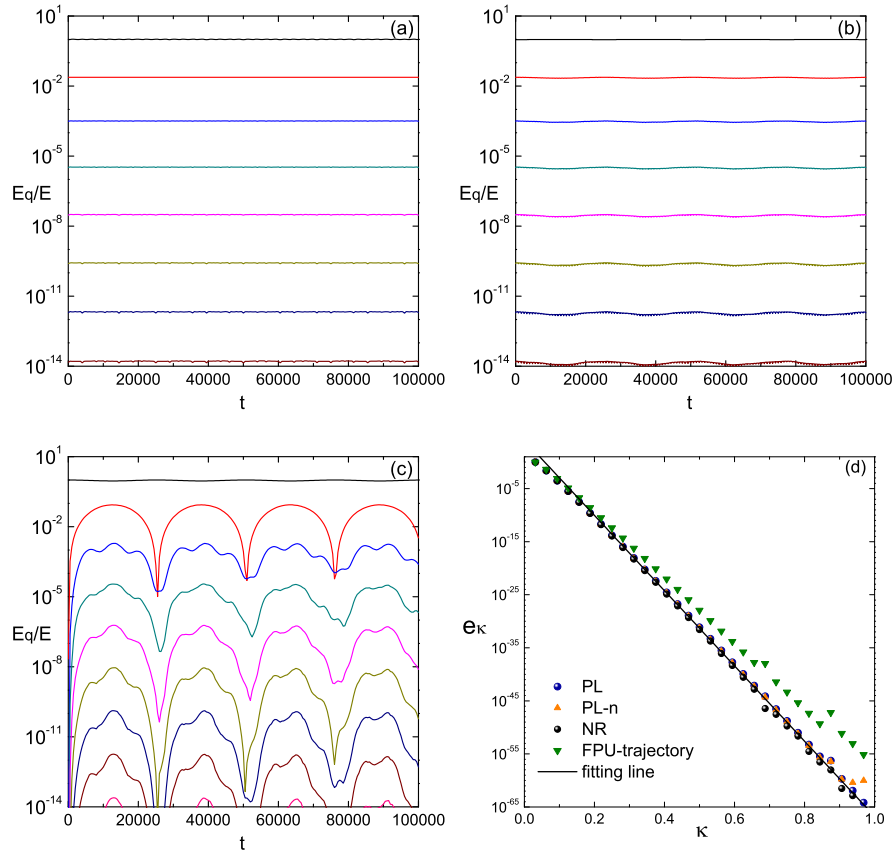


Figure 6: FPU- α system with $\alpha = 0.33$, $N = 32$ and $E = 0.00016635$. In Panels (a), (b) and (c) is shown the evolution of the normalized instantaneous spectra $E_q(t)/E$ of modes $q = 1, \dots, 8$ for the PL solution, the numerical integration of the initial condition $Q_q^{PL}(0)$, $P_q^{PL}(0)$ and for the FPU-trajectory respectively (E_1/E has the highest value and the rest progressively decrease). In panel (d) is the exponential profile of the normalized averaged energy spectra e_κ versus κ of panel (a) with blue spheres, of (b) with orange triangles, of (c) with green triangles, as well as the q -breather found by Newton-Raphson (NR) with black spheres. The continuous line is the fitting law (27).

and $E = 0.00016635$, for the truncation order $k_0 = 51$. The choice of ω_1 , as well as the resulting amplitude A_1 , are given in 4.

Fig.6(a),(b) and (c) shows the evolution of the normalized harmonic energies $E_q(t)/E$, for $q = 1, \dots, 8$ in three different computations. Namely, in (a) we compute $E_q(t)$ by the analytical solution $Q_q^{PL,51}(t)$ as found by the truncated PL series. In (b), we integrate numerically the initial conditions $Q_q^{PL,51}(0), P_q^{PL,51}(0)$. Finally, in (c) we consider an FPU-trajectory rising by the initial condition $x_n(0) = A_1 \sin(\pi n/N), y_n(0) = 0, n = 1, \dots, N - 1$.

The main remark, by a comparison of the three panels, is an important difference in the temporal behavior of the q -breather from that of the corresponding FPU-trajectory. Namely, the energies $E_q(t)$, $q = 1, \dots, 8$ remain practically constant in the case of the q -breather, while they behave as quasi-periodic functions in the case of the FPU-trajectory. In fact, the energies $E_q(t)$ for the latter oscillate around mean values following closely the energy values of the q -breather solution, but with an amplitude causing variations of more than one orders of magnitude.

We note that no considerable difference exists in panels (a) and (b), i.e. between the time evolution of the energies E_q computed via the analytical q -breather series solution and its numerical realization. In fact, we find that this trajectory returns to its initial conditions after the time $T = 2\pi/\omega_1$, with ω_1 specified by the PL method, up to 10 significant digits. This serves as an estimate of the overall precision in the analytic determination of the periodic orbit using PL series at the truncation order $k_0 = 51$.

An even greater precision can be reached, however, using the values $Q_q^{PL,51}(0), P_q^{PL,51}(0)$ as initial guess values for a numerical (Newton-Raphson) determination of the periodic orbit. Fig.6(d) shows a comparison of the averaged normalized energy spectra in all four computations, namely (i) $Q_q^{PL,51}(t)$, (ii) $Q_q^{PLn,51}(t)$, (iii) the FPU-trajectory, and (iv) the periodic orbit with initial conditions as determined by the Newton-Raphson. The fitting line in Fig.6(d) corresponds to the law

$$E_q = \gamma^{q-1} q^2 E_1, \quad \text{where } \gamma = \alpha^2 N^4 \varepsilon / \pi^4, \quad (27)$$

given in [4]. We conclude that, in agreement with [22], after a short transient time, the FPU-trajectory in this case acquires an energy spectrum similar to the one of the corresponding q -breather solution.

Fig.7 refers, now, to a different q -breather example, in which we choose to initially excite a mode at a randomly chosen position in q -space, namely $q_0 = 25$, in the system with $\alpha = 0.33, N = 32$ and $E = 0.00465079$. Again ω_{25} and A_{25} are found in the table of 4, while the truncation order here is $k_0 = 60$.

The sequence of mode excitations derived from Eq.(16) up to the 10-th order of perturbation theory is $q_1 = 14, q_2 = 11, q_3 = 28, q_4 = 3, q_5 = 22, q_6 = 17, q_7 = 8, q_8 = 31, q_9 = 6$, and $q_{10} = 19$.

Fig.7(a) shows the time evolution of the normalized energies $E_q(t)/E$ of the first seven modes in the sequence of excitations, namely q_0, \dots, q_6 , for the PL solutions $Q_q^{PL,60}(t)$ (blue) and their numerical realization $Q_q^{PLn,60}(t)$ (orange). Differences observed between the two solutions gradually increase (on a logarithmic scale) as we go to higher-order modes in the excitation sequence.

Fig.7(b) now shows the normalized averaged spectra for the solutions (i) $Q_q^{PL,60}(t)$, (ii) $Q_q^{PLn,60}(t)$, and (iii) an FPU-trajectory rising by the seed mode excitation $q_0 = 25$. We clearly see again that the FPU-trajectory's spectrum deviates from the q -breather's one at modes corresponding to a higher order in the excitation sequence.

3.4.1 The original FPU-trajectory: how many frequencies?

We finally discuss a q -breather constructed by PL series following an initial excitation resembling the one of the FPU-trajectory considered in the classical experiment of Fermi Pasta and Ulam in [1], that lead to the observation of the *FPU-recurrences*.

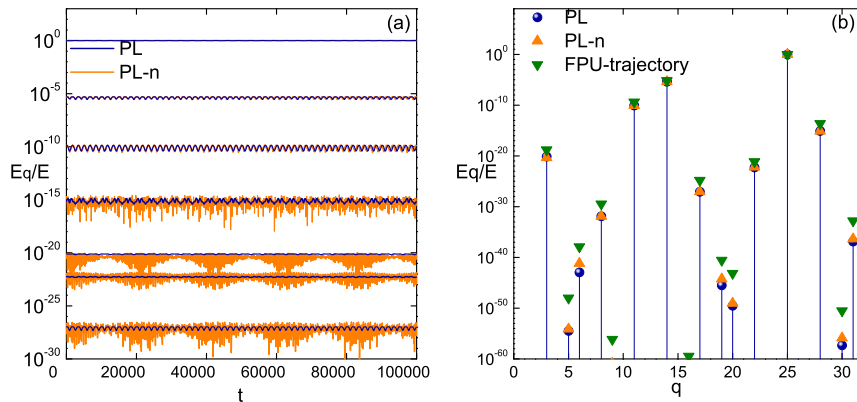


Figure 7: FPU- α system with $\alpha = 0.33$, $N = 32$, $E = 0.00465079$ with seed mode $q_0 = 25$. In panel (a) it is shown the evolution of the normalized instantaneous spectra $E_q(t)/E$ of modes 25, 14, 11, 28, 3, 22, 17 for the PL solution of the q -breather (blue) and the numerical integration (PLn) of the initial condition $Q_q^{PL}(0)$, $P_q^{PL}(0)$ (orange). In panel (b) is the exponential profile of the normalized averaged energy spectra \overline{E}_q/E versus q of PL with blue spheres, of PLn with orange triangles and of the FPU-trajectory with green triangles.

For the construction of the q -breather, we take $\alpha = 0.33$, $N = 32$ and $E = 0.014915$. The seed mode is $q_0 = 1$ and truncation order of the PL series $k_0 = 242$. The chosen frequency value ω_1 and amplitude A_1 are given in 4.

Computing the normalized energies $E_q(t)/E$, $q = 1, \dots, N - 1$ for the q -breather and the FPU-trajectory (Fig.8(a) and (b) respectively), we observe the striking difference in their time evolution. Namely, in the case of the FPU-trajectories, the energies $E_q(t)$ clearly exhibit a recursive behavior, leading to a nearly complete return to their initial values at the time $t = 12000$. On the contrary, the energies $E_q(t)$ remain practically constant for the q -breather in the same time interval. This remark is important, because it shows the difference in dynamics between two trajectories with quite similar normalized averaged spectra (Fig.8(c)).

This example clearly shows that the proximity of the averaged energy spectra cannot serve alone as a criterion for the proximity of q -breathers and FPU-trajectories in phase space. In particular, the FPU-trajectory of Fig.8 seems to evolve with more than one incommensurable frequencies, a fact implying that it lies close to a torus of dimension higher than one. By implementing the GALI method, (Fig.8(d)) we have an indication that the numerical orbit is governed by at least five incommensurable frequencies, since G_5 is the last of the GALI indicators found to asymptotically converge to a constant value (neglecting numerical fluctuations). We note, in this latter respect, that according to [14], an excitation as in Fig.8 should lead to the formation of a ‘natural packet’ of modes exhibiting a sort of internal equipartition. However, the prediction for the packet width yields $\alpha^{1/2}\varepsilon^{1/4} \simeq 2.7 \simeq 3$, which is smaller than the dimension of the torus as suggested by the GALI indicators. This fact suggests that the dimension of the packet, as found by an inspection of the energy spectra and the dimension of the underlying q -torus, need not coincide.

4 Conclusions

In the present paper, we study the dynamical features of low-dimensional invariant objects of the FPU phase space called q -tori. Our main findings can be summarized as follows:

- 1) We use the method of Poincaré – Lindstedt (PL) series in order to compute quasi-periodic series

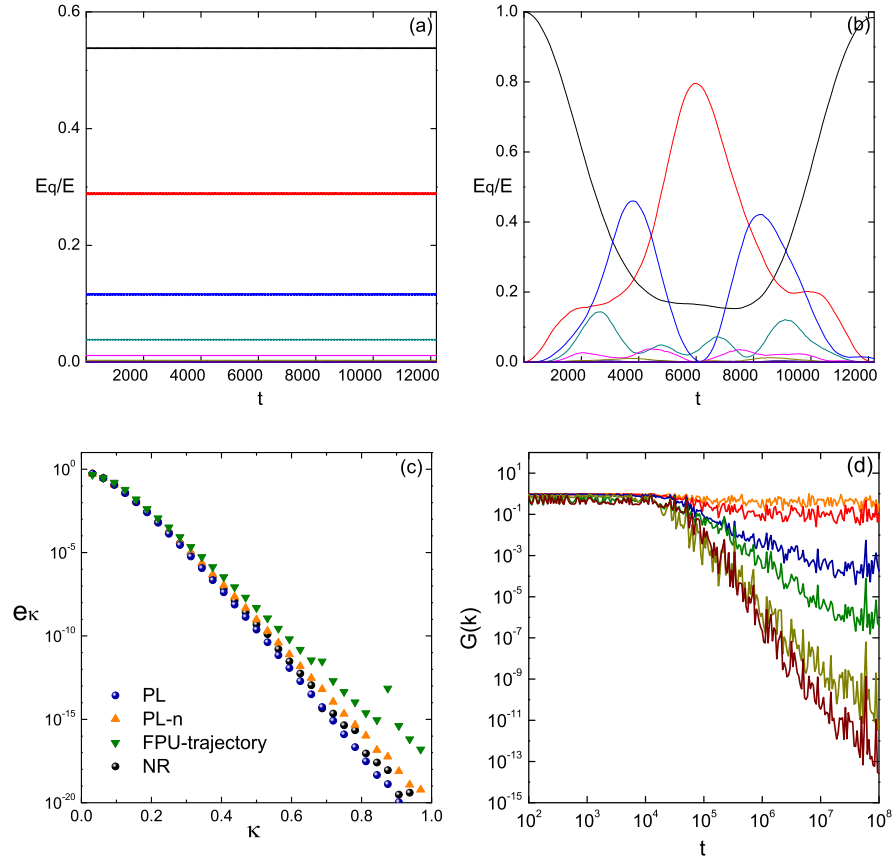


Figure 8: FPU- α with $N = 32$, $\alpha = 0.33$, $E = 0.014915$ and seed mode $q_0 = 1$. Panels (a) and (b) are for the evolution of the normalized instantaneous spectra $E_q(t)/E$ for the q -breather and the FPU-trajectory, respectively. In panel (c) is the exponential profile of the normalized averaged energy spectra e_κ of PL with blue spheres, the numerical integration (PLn) of the initial condition $Q_q^{PL}(0)$, $P_q^{PL}(0)$ with orange triangles, of FPU-trajectory with green triangles and of NR with black spheres. In (d) is the evolution of the GALI indices G_2, G_3, \dots, G_7 .

representations of trajectories approximating the motion on q -tori, up to a high order in a small parameter. We give some details on the way by which appropriate values of the torus frequencies are chosen in order for the PL method to proceed. We also discuss some numerical tests on the level of the final approximation, based on the use of the GALI indicator. An analysis of the convergence properties of the PL series is deferred to an accompanying paper [11].

2) Using properties of the PL series construction, we study the phenomenon of *energy localization* on q -tori. We present a theory of propagation of initial ‘excitations’ in the series terms. Via this theory we predict theoretically the form and shape of energy localization profiles for q -tori. Finally, we compare the latter with the energy localization profiles of orbits lying in the neighborhood of q -tori (called ‘FPU-trajectories’).

3) As a case of particular interest, we study low-frequency packet excitations. In this case, we show that q -tori solutions predict the appearance of exponential localization profiles, with a slope depending logarithmically on the system’s parameter $\alpha^{1/2}\varepsilon^{1/4}$ in the α model and on $\beta\varepsilon$ in the β . Furthermore, the q -tori exhibit invariant profiles with respect to increasing the energy E proportionally to N . Thus, the normalized energy spectra are invariant with respect to the re-scaled wavenumber $\kappa = q/N$, as long as the fraction of modes excited s/N and the specific energy are kept constant. Via leading order estimates in the PL series, we derive a law for the slope of the exponential energy profile, both in the FPU- α and FPU- β models. This turns out to be similar to that of q -breather solutions in which the ‘seed mode’ q_0 is allowed to vary proportionally to N . In fact, such laws suggest the invariance of the q -tori’s localization profiles as we approach towards the thermodynamic limit, provided that s/N and specific energy ε are kept constant. However, the existence of q -tori as $N \rightarrow \infty$ is still an open issue, as we have no proof of the convergence of the PL series in a finite domain of initial conditions as we approach this limit.

4) Regarding the FPU-trajectories lying in the neighborhood of q -tori solutions, we find that they exhibit energy localization phenomena leading to an averaged energy spectrum tending to saturate to a form quite close to that of a q -torus solution with similar initial excitation. We find that the process of energy transfer in FPU-trajectories corresponds to the so-called ‘first stage’ of the FPU dynamics in [22]. Furthermore, we provide numerical evidence that the groups of modes involved in this process are the same as the groups defined by the sets \mathcal{D}_k for q -tori. A theoretical interpretation of this phenomenon remains an open question.

As a final remark, we note that the time for which ‘metastable states’ of FPU-trajectories started close to q -tori persist, as well as its dependence on the system’s parameters, is an interesting open question that can be considered as complementary to the study in [19] (where the initially excited packet is smaller than the natural one). This is proposed as a subject for future study.

Acknowledgments We wish to thank A. Ponno and G. Benettin for their useful discussions clarifying particular points of the paper. H.C. gratefully acknowledges the hospitality of the Dipartimento di Matematica Pura e Applicata, Università di Padova, during the period May 2010 to May 2012, where this work was initiated and completed.

APPENDIX

A. Algorithm of determination of frequency values for the PL series construction

We give an iterative algorithm of determination of numerical values of the frequencies ω_{q_i} , $q_i \in \mathcal{D}_0$, for a q -torus solution with initial excitation \mathcal{D}_0 , such that the solution constructed at every step corresponds to a higher specific energy than the solution constructed in the previous step. The algorithm consists of the following steps:

Initialization. i) We choose some value of ‘trial amplitudes’ $A_{q_i}^{trial}$ and define

$$\epsilon_{l,trial} = \frac{1}{N} \sum_{i=1}^s \frac{1}{2} \Omega_{q_i}^2 A_{q_i,trial}^2, \quad q_i \in \mathcal{D}^{(0)}, \quad i = 1, \dots, s. \quad (28)$$

ii) We compute ‘trial’ frequencies by the lowest-order frequency correction terms in the series (10) corresponding to the trial amplitudes $A_{q_i,trial}$.

In the FPU- α , where the frequencies ω_{q_i} appear in the denominators of the lowest order terms, we implement a two-step substitution-iteration procedure. Namely we set

$$\begin{aligned} \omega_{q,mid}^{(2)} &= -\frac{\Omega_q}{4} \sum_{m \in \mathcal{D}_0 \cup \mathcal{D}_1} \Omega_m^2 \times \left[\Omega_q^2 A_{q,trial}^2 B_{mq}^2 \left(\frac{1}{\Omega_m^2 - 4\Omega_q^2} + \frac{2}{\Omega_m^2} \right) \right. \\ &\quad \left. + \sum_{\substack{n \in \mathcal{D}_0, n \neq q \\ \sigma^{(2)} \in \Sigma^2}} \Omega_n^2 A_{n,trial}^2 \left(\frac{2B_{qnm}^2}{\Omega_m^2 - (\sigma_1 \Omega_q + \sigma_2 \Omega_n)^2} + \frac{B_{qqm} B_{mnn}}{\Omega_m^2 - (\sigma_1 \Omega_n + \sigma_2 \Omega_n)^2} \right) \right] \end{aligned}$$

for $q \in \mathcal{D}^{(0)}$, or

$$\omega_{q,mid}^{(2)} = 0$$

for $q \notin \mathcal{D}^{(0)}$, and determine $\omega_{q,mid} = \Omega_q + \mu^2 \omega_{q,mid}^{(2)}$ for all $q = 1, \dots, N$. Then we compute

$$\begin{aligned} \omega_{q,trial}^{(2)} &= -\frac{\Omega_q}{4} \sum_{m \in \mathcal{D}_0 \cup \mathcal{D}_1} \Omega_m^2 \times \left[\Omega_q^2 A_{q,trial}^2 B_{mq}^2 \left(\frac{1}{\omega_{m,mid}^2 - 4\omega_{q,mid}^2} + \frac{2}{\omega_m^2} \right) \right. \\ &\quad \left. + \sum_{\substack{n \in \mathcal{D}_0, n \neq q \\ \sigma^{(2)} \in \Sigma^2}} \Omega_n^2 A_{n,trial}^2 \left(\frac{2B_{qnm}^2}{\omega_{m,mid}^2 - (\sigma_1 \omega_{q,mid} + \sigma_2 \omega_{n,mid})^2} + \frac{B_{qqm} B_{mnn}}{\omega_{m,mid}^2 - (\sigma_1 \omega_{n,mid} + \sigma_2 \omega_{n,mid})^2} \right) \right]. \end{aligned}$$

and set $\omega_{q,trial} = \Omega_q + \mu^2 \omega_{q,trial}^{(2)}$.

In the FPU- β , we simply have

$$\omega_{q,trial} = \Omega_q + \mu \omega_q^{(1)}(A_{q_1,trial}, \dots, A_{q_s,trial}) \quad . \quad (29)$$

iii) We compute the PL series for the excitation \mathcal{D}_0 , using as frequency values $\omega_{q_i} = \omega_{q_i,trial}$. We attempt to determine numerically a root of Eqs.(10) for the amplitudes A_{q_i} , with a root-finding technique

starting by $A_{q_i,trial}$ as guess amplitudes. If this fails, we return to substep (i), trying some lower value for the amplitudes $A_{q_i,trial}$, until a successful solution is found. We store the pairs (ω_{q_i}, A_{q_i}) of the latter.

iv) we repeat the process (i) to (iii) for some neighboring trial amplitudes $A'_{q_i,trial}$ and store the pairs $(\omega'_{q_i}, A'_{q_i})$ for the corresponding solution. We define $\Delta\epsilon_l = \epsilon'_{l,trial} - \epsilon_{l,trial}$.

Iteration. i) We define

$$\Delta\omega = \left(\sum_{i=1}^s (\omega_{q_i} - \omega'_{q_i})^2 \right)^{1/2}, \quad (30)$$

and denote by $(\omega_{q_i,0}, A_{q_i,0})$ the original solution (ω_{q_i}, A_{q_i}) .

ii) We compute s neighboring solutions corresponding to the set of frequencies $\omega_{q_i,j} = \omega_{q_i} + \delta_{ij}\Delta\omega$.

iii) We compute the matrix $J_\omega = J_A^{-1}$, where J_A is a matrix defined by the finite differences

$$J_{A,ij} = \frac{A_{q_i,j}^2 - A_{q_i,0}^2}{\Delta\omega}. \quad (31)$$

iv) Finally, we compute the next set of frequencies to be used in PL series construction by

$$\omega'_{q_i} = \omega_{q_i} + \frac{2N\Delta\epsilon_l}{s} \sum_{j=1}^s \frac{J_{\omega,ij}}{\Omega_{q_j}^2}. \quad (32)$$

This completes one full step of the iterative algorithm of determination of frequencies. We note that a change of the frequencies as in Eq.(32) leads to an increment of the total energy corresponding to each successive step by an amount of order $\Delta\epsilon_l$.

B. Proof of the proposition of subsection 2.3

We give the proof of the proposition of subsection 2.3 in the case of the FPU- α model (see [10] for the proof in the case of the FPU- β model).

The proof follows by induction. Let M_k be the set defined in Eq.(14), which corresponds to the set of all modes for which the r.h.s. of Eq.(11) is non-zero at the k -th order. According to Definition 1, the set of modes excited at the k -th order is given by $\mathcal{D}_k = M_k \setminus \bigcup_{0 \leq j \leq k-1} \mathcal{D}_j$, where $r(k) = k+1$. For $k=1$, the r.h.s. of Eq.(11) is non-zero if $B_{q_1q_2} \neq 0$, implying that for all modes $q \in M_k$ we have that q is either of the form $q = |\sigma^{(2)}q^{(2)}|$, or of the form $q = |2N - |\sigma^{(2)}q^{(2)}||$, where the allowable combinations of values of $q^{(2)} = (q_1, q_2) \in \mathcal{D}_0^2$ and of $\sigma^{(2)} = (\sigma_1, \sigma_2) \in \Sigma^2$, are those leading to $1 \leq q \leq N-1$.

Assuming, now, the proposition to be true at order $k-1$, one finds that, at the k -th order, the r.h.s. of Eq.(11) is non-zero if $B_{qlm} \neq 0$, $Q_l^{(n_1)} \neq 0$ and $Q_m^{(n_2)} \neq 0$, where $n_1 + n_2 = k-1$. For the modes $l \in M_{n_1}$ and $m \in M_{n_2}$ we then have:

$$l = \left| 2\nu_1 N - |\sigma^{(n_1+1)}q^{(n_1+1)}| \right|, \quad m = \left| 2\nu_2 N - |\sigma^{(n_2+1)}q^{(n_2+1)}| \right|,$$

where $\nu_i = \left\lfloor \frac{|\sigma^{(n_i+1)}q^{(n_i+1)}| + N - 1}{2N} \right\rfloor$. However, the condition $B_{qlm} \neq 0$ implies that q is necessarily of the form $q = |l \pm m|$ or $q = |2N - |l \pm m||$. Provided that $1 \leq q \leq N-1$, the two latter equations can be written in a combined form as:

$$q = |2Ng - |l \pm m|| \quad (33)$$

where $g = 0$ or 1 . Then, Eq.(33) takes the form

$$\begin{aligned} q &= |2Ng \pm 2\nu_1 N \pm 2\nu_2 N \mp | \sigma^{(n_1+1)} q^{(n_1+1)} | \mp | \sigma^{(n_2+1)} q^{(n_2+1)} | | \\ &= |2N(\underbrace{|g \pm \nu_1 \pm \nu_2|}_{\nu}) - | \sigma^{(k+1)} q^{(k+1)} | |, \end{aligned} \quad (34)$$

after a possible sign reversal within $|\cdot|$ (not affecting the absolute value) and with ν a positive integer.

However, by the restriction $1 \leq q \leq N-1$, one necessarily has that $\nu = [(| \sigma^{(k+1)} q^{(k+1)} | + N - 1)/2N]$. This concludes the proof of the proposition.

C. The mapping $\mathcal{K}_q^{(k)}$ for FPU $-\alpha$

We give the expressions of the quantities appearing in the mapping (19), up to the order $k = 3$. We have

$$\begin{aligned} \mathcal{K}_{q_1; \alpha}^{(1)} &= B_{q_1 q_0 q_0} \\ \mathcal{K}_{q_2; \alpha}^{(2)} &= 2\mathfrak{L}_{q_0}^{(0)} \mathfrak{L}_{q_1}^{(1)} \mathcal{K}_{q_0}^{(0)} \mathcal{K}_{q_1}^{(1)} B_{q_2 q_1 q_0} = 2 \frac{\Omega_{q_1}^2}{\Omega_{q_1}^2 - (\sigma_1 \omega_{q_0} + \sigma_2 \omega_{q_0})^2} B_{q_1 q_0 q_0} B_{q_2 q_1 q_0} \\ \mathcal{K}_{q_3; \alpha}^{(3)} &= 2\mathfrak{L}_{q_0}^{(0)} \mathfrak{L}_{q_2}^{(2)} \mathcal{K}_{q_0}^{(0)} \mathcal{K}_{q_2}^{(2)} B_{q_3 q_2 q_0} + [\mathfrak{L}_{q_1}^{(1)} \mathcal{K}_{q_1}^{(1)}]^2 B_{q_3 q_1 q_1} = \\ &4 \frac{\Omega_{q_1}^2 \Omega_{q_2}^2 B_{q_1 q_0 q_0} B_{q_2 q_1 q_0} B_{q_3 q_2 q_0}}{[\Omega_{q_1}^2 - (\sigma_1 \omega_{q_0} + \sigma_2 \omega_{q_0})^2][\Omega_{q_2}^2 - (\sigma_1 \omega_{q_0} + \sigma_2 \omega_{q_0} + \sigma_3 \omega_{q_0})^2]} \\ &+ \left[\frac{\Omega_{q_1}^2 B_{q_1 q_0 q_0}}{\Omega_{q_1}^2 - (\sigma_1 \omega_{q_0} + \sigma_2 \omega_{q_0})^2} \right]^2 B_{q_3 q_1 q_1}, \end{aligned}$$

where q_0, q_1, q_2 and q_3 represent any mode belonging in the sets $\mathcal{D}_0, \mathcal{D}_1, \mathcal{D}_2$ and \mathcal{D}_3 respectively.

D. Explicit expressions for the leading order terms of the PL series

We prove by induction that the leading order terms $Q_q^{(k)}$ for the modes $q \in \mathcal{D}_k$ are given by Eqs. (17) with the quantities $\mathcal{R}_q^{(k)}, \mathcal{K}_q^{(k)}$ given by (18), (19) and (20). We focus again on the FPU $-\alpha$ model.

For $k = 1$, the solutions of Eqs.(11) read

$$Q_q^{(1)}(t) = -\frac{\Omega_q}{4} \sum_{\substack{n^{(2)} \in \mathcal{D}_0^{(2)} \\ \sigma^2 \in \Sigma^2}} \Omega_{n_1} \Omega_{n_2} A_{n_1} A_{n_2} B_{q n_1 n_2} \frac{e^{i(\sigma_1 \omega_{n_1} + \sigma_2 \omega_{n_2})t}}{\Omega_q^2 - (\sigma_1 \omega_{n_1} + \sigma_2 \omega_{n_2})^2} \quad (35)$$

so, $Q_q^{(1)}$ satisfies Eq.(17).

Assume now that Eq.(17) holds true for the solution $Q_q^{(k)}(t)$ at the order $k-1$. For simplicity, we use the notation $\mathcal{R}_l^{(n_i)} = \mathcal{R}_l^{(n_i)}(n^{(r(n_i))})$ and $\mathcal{K}_l^{(n_i)} = \mathcal{K}_l^{(n_i)}(n^{(r(n_i))})$, $i = 1, \dots, r(k)$. At order k , Eq. (11) takes the form

$$\begin{aligned} \ddot{Q}_q^{(k)} + \Omega_q^2 Q_q^{(k)} &= \\ -\Omega_q \sum_{m_1, m_2=1}^{N-1} \Omega_{m_1} \Omega_{m_2} B_{q m_1 m_2} \sum_{\substack{l_{1,2}=0 \\ l_1+l_2=k-1}}^{k-1} \sum_{\substack{n^{(r(k))} \in \mathcal{D}_0^{r(k)} \\ \sigma^{(r(k))} \in \Sigma^{r(k)}}} \mathcal{R}_{m_1}^{(l_1)} \mathcal{R}_{m_2}^{(l_2)} \mathcal{K}_{m_1}^{(l_1)} \mathcal{K}_{m_2}^{(l_2)} e^{i\sigma^{(r(k))} \omega_n^{(r(k))} t}. \end{aligned} \quad (36)$$

By replacing the term

$$\begin{aligned}\mathcal{R}_{m_1}^{(l_1)}\mathcal{R}_{m_2}^{(l_2)} &= \frac{(-1)^{l_1+l_2}}{2^{r(l_1)+r(l_2)}} \cdot \frac{\mathfrak{L}_{m_1}^{(l_1)}\mathfrak{L}_{m_2}^{(l_2)}}{\Omega_{m_1}\Omega_{m_2}} \cdot \Omega_{n_1} \dots \Omega_{n_{r(k)}} A_{n_1} \dots A_{n_{r(k)}} \\ &= -\frac{\mathfrak{L}_{m_1}^{(l_1)}\mathfrak{L}_{m_2}^{(l_2)}}{\Omega_{m_1}\Omega_{m_2}} \cdot \frac{\Omega_q^2 - (\sigma^{(r(k))}\omega_n^{(r(k))})^2}{\Omega_q} \cdot \mathcal{R}_q^{(k)}\end{aligned}\quad (37)$$

into the above equation, one has that

$$\begin{aligned}\ddot{Q}_q^{(k)} + \Omega_q^2 Q_q^{(k)} &= (\Omega_q^2 - (\sigma^{(r(k))}\omega_n^{(r(k))})^2) \\ &\times \sum_{\substack{n^{(r(k))} \in \mathcal{D}_0^{r(k)} \\ \sigma^{(r(k))} \in \Sigma^{r(k)}}} \mathcal{R}_q^{(k)} \left(\sum_{\substack{l_1, l_2=0 \\ l_1+l_2=k-1}}^{k-1} \sum_{m_1, m_2=1}^{N-1} \mathfrak{L}_{m_1}^{(l_1)}\mathfrak{L}_{m_2}^{(l_2)}\mathcal{K}_{m_1}^{(l_1)}\mathcal{K}_{m_2}^{(l_2)}B_{qm_1m_2} \right) e^{i\sigma^{(r(k))}\omega_n^{(r(k))}t} \\ &= (\Omega_q^2 - (\sigma^{(r(k))}\omega_n^{(r(k))})^2) \sum_{\substack{n^{(r(k))} \in \mathcal{D}_0^{r(k)} \\ \sigma^{(r(k))} \in \Sigma^{r(k)}}} \mathcal{R}_q^{(k)}\mathcal{K}_q^{(k)} e^{i\sigma^{(r(k))}\omega_n^{(r(k))}t}.\end{aligned}\quad (38)$$

However, the solution of the latter equation is

$$Q_q^{(k)}(t) = \sum_{\substack{n^{(r(k))} \in \mathcal{D}_0^{r(k)} \\ \sigma^{(r(k))} \in \Sigma^{r(k)}}} \mathcal{R}_q^{(k)}\mathcal{K}_q^{(k)} e^{i\sigma^{(r(k))}\omega_n^{(r(k))}t}.\quad (39)$$

Thus, Eq.(17) holds true at the order k , with the expressions $\mathcal{R}_q^{(k)}$, $\mathcal{K}_q^{(k)}$ given by (18), (19) and (20).

E. Localization profiles of q -tori estimated by leading order terms in the PL series

We derive estimates for the form of the energy localization profiles for q -tori solutions corresponding to an initial excitation of the modes $1 \leq q \leq s$, with s varying proportionally to N .

We first make the following estimates:

i) For any mode $q \in \mathcal{D}_k$ we use the approximation $q \simeq c_k s$, where $c_k s$ is the mid mode of \mathcal{D}_k , i.e. $q = ks + [s/2]$ ($c_k \simeq k + 1/2$) in FPU- α and $q = 2ks$ ($c_k = 2k$) in FPU- β .

ii) For the unperturbed frequencies we use the approximation $\Omega_q \simeq \pi q/N$.

iii) For $m \in \mathcal{D}_k$ and for ‘almost resonant terms’, for which $m - \sigma^{(r(k))}n = 0$, we use the approximation $|\Omega_m - \sigma^{(r(k))}\omega_n^{(r(k))}| \simeq \pi^3 m^3 / (24N^3)$ (See Appendix B of [10] for its derivation).

iv) For the quantities $\mathfrak{L}_m^{(k)}$ of Eq.(21) we set

$$|\mathfrak{L}_m^{(k)}(n^{(r(k))})| \simeq \frac{\Omega_m}{2[\Omega_m - \sigma^{(r(k))}\omega_n^{(r(k))}]} \sim \frac{12N^2}{\pi^2 m^2}$$

v) Finally, for the total energy of the system we use the approximation $E \simeq \sum_{n=1, \dots, s} E_n$, where $E_n \simeq 1/2 A_n^2 \Omega_n^2$.

We will now derive an estimate for the quantity $|Q_q^{(k)}|$ of Eq.(17). We first write some approximations for the terms of Eqs.(18), (19) and (20). Recalling that $r(k) = k + 1$ in the α model, and $r(k) = 2k + 1$ in β , and taking into account the approximations (i)–(v), we find

$$|\mathcal{R}_q^{(k)}| \simeq \frac{\Omega_q}{\Omega_q^2 - (\sigma^{(r)}\omega_n^{(r)})^2} \cdot \Omega_{n_1} \dots \Omega_{n_r} A_{n_1} \dots A_{n_r} \sim \frac{12N^3}{\pi^3 q^3} \cdot \left(\frac{2E}{s}\right)^{r(k)/2}.\quad (40)$$

The quantities $\mathcal{K}_{q;\alpha}^{(k)}$ and $\mathcal{K}_{q;\beta}^{(k)}$ of (19) and (20) cannot be evaluated analytically. However, as already mentioned in section 2.4, their form is a polynomial of degree $k - 1$ in the terms $\mathfrak{L}_m^{(l)}$, $l = 0, 1, \dots$ and a polynomial of degree k in $B_{q,l,m}$ (or $C_{q,l,m,n}$). We denote here by $\mathcal{P}(q, n^{(r)}, m^{(k-1)})$ the product of k factors of the coefficients $B_{q,l,m}$ (or $C_{q,l,m,n}$) in $\mathcal{K}_{q;\alpha}^{(k)}$ (or $\mathcal{K}_{q;\beta}^{(k)}$).

The size of the mid mode is then

$$\begin{aligned}
A_q^{(k)} &\sim |Q_q^{(k)}| \sim \sum_{\substack{n^{(r)} \in \mathcal{D}_0^r \\ \sigma^{(r)} \in \Sigma^r}} |\mathcal{R}_q^{(k)}| \cdot |\mathcal{K}_q^{(k)}| \\
&\sim |\mathcal{R}_q^{(k)}| \cdot C_k \sum_{\substack{n^{(r)} \in \mathcal{D}_0^r \\ \sigma^{(r)} \in \Sigma^r}} \sum_{\substack{m_i \in \mathcal{D}_{l_i} \\ i=1, \dots, k-1}} |\mathfrak{L}_{m_1}^{(l_1)}| |\mathfrak{L}_{m_2}^{(l_2)}| \dots |\mathfrak{L}_{m_{k-1}}^{(l_{k-1})}| \mathcal{P}(q, n^{(r)}, m^{(k-1)}) \\
&\sim |\mathcal{R}_q^{(k)}| \cdot C_k \cdot \left(\frac{12N^2}{\pi^2} \right)^{k-1} \sum_{\substack{n^{(r)} \in \mathcal{D}_0^r \\ \sigma^{(r)} \in \Sigma^r}} \sum_{\substack{m_i \in \mathcal{D}_{l_i} \\ i=1, \dots, k-1}} \frac{1}{(m_1 \dots m_{k-1})^2} \mathcal{P}(q, n^{(r)}, m^{(k-1)}) \quad , \quad (41)
\end{aligned}$$

where by C_k we note constants in powers of k . Due to the term $\mathcal{P}(q, n^{(r)}, m^{(k-1)})$, the sums over $n^{(r)}$ and $m^{(k-1)}$ in (41) give rise to a factor $s^{(r(k)+1)/2}$, i.e. $s^{k/2+1}$ in α and to s^{k+1} in β ⁴. Replacing m_i , $i = 1, \dots, k - 1$ and q in (41) by their mid mode expression $c_k s$, one has

$$\begin{aligned}
A_q^{(k)} &\simeq C'_k \frac{12N^3}{\pi^3 q^3} \cdot \left(\frac{2E}{s} \right)^{r(k)/2} s^{(r(k)+1)/2} \left(\frac{12N^2}{\pi^2 s^2} \right)^{k-1} \\
&= C''_k \frac{N^{2k+1}}{\pi^{2k+1} s^{2k+1}} E^{r(k)/2} \quad . \quad (42)
\end{aligned}$$

The energy in each group of modes is then estimated as

$$\begin{aligned}
E^{(k)} &\simeq \frac{1}{2} \mu^{2k} \Omega_q^2 A_q^2 \simeq \frac{1}{2} \mu^{2k} \left(\frac{\pi c_k s}{N} \right)^2 \cdot \left(C''_k \frac{N}{\pi s} \right)^{2(2k+1)} E^{r(k)} \\
&\simeq C'''_k \cdot \left(\frac{\mu N^2}{\pi^2 s^2} \right)^{2k} E^{r(k)} \quad . \quad (43)
\end{aligned}$$

Finally, replacing $r(k)$ and μ by $k+1$ and $\alpha/\sqrt{2N}$ for FPU- α , or $2k+1$ and $\beta/(2N)$ for FPU- β respectively, we arrive at the exponential laws

$$\begin{aligned}
E_\alpha^{(k)} &\sim C'''_k \cdot \left(\frac{\alpha^2 E N^3}{\pi^4 s^4} \right)^k \sim \left(\frac{\alpha^2 \varepsilon N^4}{\pi^4 s^4} \right)^k \\
E_\beta^{(k)} &\sim C'''_k \cdot \left(\frac{\beta^2 E^2 N^2}{\pi^4 s^4} \right)^k \sim \left(\frac{\beta^2 \varepsilon^2 N^4}{\pi^4 s^4} \right)^k \quad . \quad (44)
\end{aligned}$$

F. Precise values of frequencies and amplitudes in all paper's numerical examples

⁴ These factors are found by recursively solving $\sum_{\substack{n^{(r)} \in \mathcal{D}_0^r \\ \sigma^{(r)} \in \Sigma^r}} \mathcal{P}(q, n^{(r)}, m^{(k-1)})$, for those q and $m^{(k-1)}$ that maximize the results. In β one finds for $k = 1$ the factor $2s(s - 1)$, for $k = 2$ the factor $4s^2(s - 1)$, etc.

Example	Frequencies	Amplitudes
Fig.1, $\mathcal{D}_0 = \{1, 2, 3, 4\}$	$\omega_1 = 0.09813690483108113$ $\omega_2 = 0.19603499627351076$ $\omega_3 = 0.29346131418681830$ $\omega_4 = 0.39018079936090050$	$A_1 = 0.098097447281306230$ $A_2 = 0.048959912346992665$ $A_3 = 0.032444239210574590$ $A_4 = 0.023892612612360370$
Fig.4a, $\mathcal{D}_0 = \{1, 11, 21, 31\}$	$\omega_1 = 0.09814720863898445$ $\omega_{11} = 1.0282023436963477$ $\omega_{21} = 1.7154505429645952$ $\omega_{31} = 1.9975829222954775$	$A_1 = 0.2699420271816366000$ $A_{11} = 0.027437337334704704$ $A_{21} = 0.015901830855243902$ $A_{31} = 0.014550407721151376$
Fig.4b, $\mathcal{D}_0 = \{60, 61, 62, 63\}$	$\omega_{60} = 1.9903455323483594$ $\omega_{61} = 1.9945569202421924$ $\omega_{62} = 1.9975668544869103$ $\omega_{63} = 1.9993735255838023$	$A_{60} = 0.010626655362545707$ $A_{61} = 0.010540492500677328$ $A_{62} = 0.010486090307194270$ $A_{63} = 0.010462240436802113$
Fig.4c, $\mathcal{D}_0 = \{63, 64, 65\}$	$\omega_{63} = 1.3967520180075357$ $\omega_{64} = 1.4142130013133483$ $\omega_{65} = 1.4314611496716776$	$A_{63} = 0.005128073559888574$ $A_{64} = 0.005045052412361571$ $A_{65} = 0.004963639646819611$
Fig.4d, $\mathcal{D}_0 = \{94, \dots, 98\}$	$\omega_{94} = 1.8284112766464593$ $\omega_{95} = 1.8382194182395468$ $\omega_{96} = 1.8477507307792000$ $\omega_{97} = 1.8570037790005570$ $\omega_{98} = 1.8659771693147402$	$A_{94} = 0.008845316872292220$ $A_{95} = 0.008752766020034742$ $A_{96} = 0.008700391793859069$ $A_{97} = 0.008662026577864702$ $A_{98} = 0.008661383820872627$
Fig.6, $\mathcal{D}_0 = \{1\}$	$\omega_1 = 0.09814109959448596$	$A_1 = 0.18574105489382606$
Fig.7, $\mathcal{D}_0 = \{25\}$	$\omega_{25} = 1.8830741847088537$	$A_{25} = 0.0512142216322969$
Fig.8, $\mathcal{D}_0 = \{1\}$	$\omega_1 = 0.09844127049688513$	$A_1 = 1.3009149083500795$

References

- [1] E. Fermi, J. Pasta, and S. Ulam, Los Alamos report No LA-1940 (1955) 977.
- [2] R. L. Bivins, N. Metropolis, and J. Pasta, J. Comp. Phys. **12** (1973) 65.
- [3] S. Flach, M. V. Ivanchenko, and O. I. Kanakov, Phys. Rev. Lett. **95** (2005) 064102.
- [4] S. Flach, M. V. Ivanchenko, and O. I. Kanakov, Phys. Rev. E **73** (2006) 036618.
- [5] M. V. Ivanchenko, O. I. Kanakov, K. G. Mishagin, and S. Flach, Phys. Rev. Lett. **97** (2006) 025505.
- [6] S. Flach and A. Ponno, Physica D **237** (2008) 908.
- [7] S. Flach, O. Kanakov, M. Ivanchenko, and K. Mishagin, Int. J. Mod. Phys. B **21** (2007) 3925.
- [8] O. Kanakov, S. Flach, M. Ivanchenko, and K. Mishagin, Phys. Lett. A **365** (2007) 416.
- [9] S. Flach and T. Penati, Chaos **17** (2007) 023102.

- [10] H. Christodoulidi, C. Efthymiopoulos and T. Bountis, *Phys. Rev. E* **81** (2010) 016210.
- [11] C. Efthymiopoulos, H. Christodoulidi, in preparation, (2012).
- [12] F. Fucito, F. Marchesoni, E. Marinari, G. Parisi, L. Politi, S. Ruffo, and A. Vulpiani, *J. Physique* **43** (1982) 707.
- [13] R. Livi, M. Pettini, S. Ruffo, and A. Vulpiani, *Phys. Rev. A* **31** (1985) 2740.
- [14] L. Berchialla, A. Giorgilli, and S. Paleari, *Phys. Lett. A* **321** (2004) 167.
- [15] J. D. Luca, A. J. Lichtenberg, and S. Ruffo, *Phys. Rev. E* **60** (1999) 3781.
- [16] A. Lichtenberg, R. Livi, M. Pettini, and S. Ruffo, *Lect. Notes Phys.* **728** (2008) 21.
- [17] L. Berchialla, L. Galgani, and A. Giorgilli, *Discr. Cont. Dyn. Sys. A* **11** (2005) 855.
- [18] T. Genta, A. Giorgilli, S. Paleari, and T. Penati, *Phys. Lett. A* **376** (2012) 2038.
- [19] G. Benettin and A. Ponno, *J. Stat. Phys.* **144** (2011) 793.
- [20] A. Ponno and D. Bambusi, *Chaos* **15** (2005) 015107.
- [21] D. Bambusi and A. Ponno, *Comm. Math. Phys.* **264** (2006) 539.
- [22] A. Ponno, H. Christodoulidi, Ch. Skokos and S. Flach, *Chaos* **21** (2011) 043127.
- [23] C. Skokos, T. Bountis, and C. Antonopoulos, *Physica D* **231** (2007) 30.
- [24] H. Christodoulidi and T. Bountis, *Romai J.* **2** (2006) 37.
- [25] C. Skokos, T. Bountis, and C. Antonopoulos, *Eur. Phys. J. Special Topics* **165** (2008) 5.
- [26] P. Hemmer, Dynamic and stochastic type of motion by the linear chain. *Det Physiske Seminar i Trondheim* **2** (1959) 66.
- [27] P. Poggi and S. Ruffo, *Physica D* **103** (1997) 251.
- [28] B. Rink, *Physica D* **175** (2003) 31.
- [29] G. M. Chechin, D. S. Ryabov, and K. G. Zhukov, *Physica D* **203** (2005) 121.